

# Time Variant Reliability Analysis of Nonlinear Structural Dynamical Systems using combined Monte Carlo Simulations and Asymptotic Extreme Value Theory

B Radhika<sup>1</sup>, S S Panda<sup>1</sup> and C S Manohar<sup>1,2</sup>

**Abstract:** Reliability of nonlinear vibrating systems under stochastic excitations is investigated using a two-stage Monte Carlo simulation strategy. For systems with white noise excitation, the governing equations of motion are interpreted as a set of Ito stochastic differential equations. It is assumed that the probability distribution of the maximum in the steady state response belongs to the basin of attraction of one of the classical asymptotic extreme value distributions. The first stage of the solution strategy consists of selection of the form of the extreme value distribution based on hypothesis tests, and the next stage involves the estimation of parameters of the relevant extreme value distribution. Both these stages are implemented using data from limited Monte Carlo simulations of the system response. The proposed procedure is illustrated with examples of linear/nonlinear systems with single/multiple degrees of freedom, driven by random excitations. The predictions from the proposed method are compared with the results from large scale Monte Carlo simulations, and also with the classical analytical results, when available, from the theory of out-crossing statistics. Applications of the proposed method for large-scale problems and for vibration data obtained from field/laboratory conditions, are also discussed.

## 1 Introduction

Reliability analysis of nonlinear structural dynamical systems under random excitation has remained one of the most difficult problems

in structural safety analysis. These problems lie at the heart of structural design against extreme loads such as those due to earthquakes and extreme winds. In these problems one seeks to evaluate the probability that a specified response quantity remains below a specified level in a given time duration. Thus, if  $X(t)$  is the response of the random process of interest,  $\alpha$  is the acceptable limit and  $(0, T)$  is the given time duration, we seek to evaluate the probability  $P[X(t) < \alpha \forall t \in (0, T)]$ . This time variant form of reliability evaluation could be replaced by a time invariant form given by  $P\left[\max_{t \in (0, T)} \{X(t)\} < \alpha\right] = P[X_m < \alpha]$  where  $X_m = \max_{t \in (0, T)} X(t)$  is the extreme value of the process  $X(t)$  over  $(0, T)$ . The determination of the probability distribution function (PDF) of  $X_m$  constitutes an important step. Exact analytical solutions to determine of PDF of  $X_m$  are rarely possible even for problems in linear mechanics. The main sources of difficulty associated with determination of the probability of failure of dynamical systems are the following:

- $X(t)$  could be non-Gaussian in nature (because of non-Gaussian nature of the inputs, nonlinearity in the behaviour of structural mechanics, response being nonlinear function of Gaussian processes as in evaluation of principal stresses or von Mises' stress metric, and/or due to randomness in structural parameters),
- inability to completely characterize the properties of  $X(t)$ ,
- relatively large size in terms of degrees of freedom of the dynamical system under

<sup>1</sup>Department of Civil Engineering, Indian Institute of Science, Bangalore 560 012 India. Email: manohar@civil.iisc.ernet.in

<sup>2</sup>Corresponding author. Email: manohar@civil.iisc.ernet.in

study which demand significant computational effort, and

- the desired probability  $P[\max_{t \in (0, T)} \{X(t)\} < \alpha]$  is most often a small number of the order of  $10^{-5}$  or even less.

The problem gets further complicated if more than one performance function is considered, or when issues related to epistemic uncertainties are also to be tackled. Methods of reliability analysis reported in the literature could be grouped into the following categories (Manohar and Gupta 2005): (a) methods based on Markov property of response processes, (b) out-crossing approaches combined with approximate strategies such as equivalent linearization, and (c) Monte Carlo simulations and possible refinements to achieve variance reduction.

For a white Gaussian noise input process, the response will be a diffusion process, and the associated transitional probability density function (pdf) will satisfy the well known Kolmogorov equations (Lin and Cai 1995). The formulation of these equations leads to the exact characterization of the response for a limited class of problems, which helps in formulating strategies for approximate analysis for a wider class of problems. The Markov property of the response can be used in the study of the first passage probabilities. Here, either the forward or the backward Kolmogorov equation is solved in conjunction with appropriate boundary conditions imposed along the critical barriers. Alternatively, starting from the backward Kolmogorov equation, one can also derive equations for moments of the first passage time (the generalized Pontraigin Vitt equations), which, in principle, can be solved recursively (Roberts 1986, Lin and Cai 1995). For systems that are driven by broadband random excitations, the method of stochastic averaging provides a means to approximate the response as a Markov process (Manohar 1995). Subsequently, Markovian methods can be used to study the first passage failures of such systems. This approach has been adopted in several studies (Noori *et al.*, 1995, Cai and Lin 1998 and Gan and Zhu 2001).

A recursive scheme that uses the Green's function of the forward Kolmogorov equation for the study of the first passage failure has been outlined by Sharp and Allen (1998).

In the studies based on the out-crossing approach, one begins by modeling the process that counts the number of times the response trajectory exits the safe domain, based on which the average rate of crossing of the safe domain is determined. The Poisson model is often used for this counting process. Based on this, the probability that the response remains within safe domain, within a given time duration, is established. The problem of out-crossing of scalar and vector random processes across deterministic thresholds has been widely studied in the literature. The average number of out-crossings from safe to unsafe region for a scalar random process  $x(t)$  across a time varying boundary can be derived based on the well known Rice's formula (1956). Studies on out-crossing of vector random processes from safe regions have also been made. As might be expected, exact solutions with vector random processes are possible only for limited class of problems: see, for instance, the work of Veneziano *et al.*, (1979) on vector Gaussian random process out-crossing of elliptic, spherical and polyhedral safe regions. In the context of studies on out-crossing of vector random processes, Hagen and Tvedt (1991) and Hagen (1992) explored an earlier proposition by Madsen (unpublished) that the up-crossing rate of scalar stochastic processes as a particular sensitivity measure of the failure probability associated with a suitably defined parallel system. The paper by Rackwitz (1998) documents the results available on mean rates for a set of random processes that include rectangular wave vector process, scalar and vector Gaussian random processes, and Nataf and Hermite random processes. Further details are also available in the book by Melchers (1999). The paper by Li and Ghanem (1998) employs an approximate analytical solution technique based on polynomial chaos expansion to investigate the statistics of extremes of response of a nonlinear system to random excitations. The study by Der Kiureghian (2000) offers a new perspective to problems of

random vibration involving linear/nonlinear oscillators under Gaussian/non-Gaussian random excitations. Here, the excitation process is discretized using a series representation, such as, Karhunen-Loeve expansion or stochastic Fourier series. The geometric forms of the system response in the space spanned by these discretized random variables are explored. In doing so, various forms such as vectors, planes, half-spaces, wedges and ellipsoids, are encountered depending upon the response variable studied. Application of the first order and second order reliability methods is explored in this context. The works of Leira (1994, 2004), Gupta and Manohar (2005, 2006), and Song and Der Kiureghian (2006) represent efforts to develop multivariate extreme value distributions with a view for applications in the reliability of structural systems.

Brute force Monte Carlo simulation studies are increasingly infeasible to apply, as the structural models become large and nonlinear, and also as the probability of failure becomes smaller. The idea of using simulations based on importance sampling has been explored by some authors (Pradlwarter and Schueller 1999, Bayer and Bucher 1999, Au and Beck 2001). The idea of employing response surface models has also been explored (Brenner and Bucher 1995, Yao and Wen 1996, Zhao *et al.*, 1999, Gupta and Manohar 2003, 2005). The works of Macke and Bucher (2003) and Olsen and Naess (2006) explore the use of mathematical theorems on the change of probability measure based on Girsanov theorem, and on the results from stochastic control theory for estimation of reliability of dynamical systems. Dunne and Ghanbari (2001) have studied the extreme value distribution of the dynamic response of a clamped beam subjected to band limited random noise excitation by comparing solutions from Fokker Planck equations and from the data based extreme value analysis.

In the present study we explore the possibility of combining Monte Carlo simulation with application of asymptotic theory of extreme value distributions for time variant reliability analysis of dynamical systems. The basic idea here is to carry out a limited number of Monte Carlo sim-

ulations of response processes, and based on the data so available, to select objectively an appropriate form of the asymptotic PDF of the highest response in a given time duration. Once the form of this PDF is identified, further (limited) simulations are carried out, based on which, the parameters of the PDF are identified. This enables the evaluation of the probability that the response stays within safe regions in a given time duration. The potential advantage of this approach is the ability to estimate the structural reliability with relatively small number of Monte Carlo runs. The proposed method is illustrated for oscillators with a single degree of freedom (sdof) and with multiple degrees of freedom (mdof), driven by white Gaussian noise. The reliability of a wind turbine structure subjected to dynamic effects of wind is also studied. Questions on applications of the proposed strategy when vibration data is measured in laboratory/field conditions are also addressed. The results indicate the potential of the proposed method for engineering applications. To understand the context of the present study, we first present a brief overview of the classical extreme value theory.

## 2 Extreme value theory

The classical extreme value theory of random variables considers the problem of determination of PDF of extremes of a sequence of independent identically distributed (iid) random variables  $\{X_i\}_{i=1}^n$  as  $n \rightarrow \infty$ . Here it is established that there exists only three types of non-degenerate probability distributions for  $X_m = \max_{n \rightarrow \infty} \{X_i\}_{i=1}^n$  given by (Castillo 1988).

$$\begin{aligned}
 H_{1,\gamma}(x) &= \exp(-x^{-\gamma}) && \text{for } x > 0 \\
 &= 0 && \text{otherwise} \\
 H_{2,\gamma}(x) &= 1 && \text{for } x \geq 0 \\
 &= \exp[-(-x)^\gamma] && \text{otherwise} \\
 H_{3,0}(x) &= \exp[-\exp(-x)] && -\infty < x < \infty
 \end{aligned} \tag{1}$$

These distributions are, respectively, the Frechet, Weibull and Gumbel distributions for the maxima. Similarly, for  $Y_m = \min_{n \rightarrow \infty} \{X_i\}_{i=1}^n$ , the three possible degenerate distributions are given by (Castillo

1988).

$$\begin{aligned}
 L_{1,\gamma}(x) &= 1 - \exp[-(-x)^{-\gamma}] && \text{for } x < 0 \\
 &= 1 && \text{otherwise} \\
 L_{2,\gamma}(x) &= 1 - \exp(-x^\gamma) && \text{for } x > 0 \\
 &= 0 && \text{otherwise} \\
 L_{3,0}(x) &= 1 - \exp[-\exp(x)] && -\infty < x < \infty
 \end{aligned} \tag{2}$$

These distributions are, again, respectively, the Frechet, Weibull and Gumbel distributions for the minima. In general, any iid sequence  $\{X_i\}_{i=1}^n$  with a common PDF  $F(x)$  can be viewed as belonging to the basin of attraction of one of the three extreme value distributions listed above. Theorems for determining the domain of attraction to which a given  $F(x)$  belongs has been established. The tails of  $F(x)$  play a central role in this determination. Thus, the extreme value distribution from an initial density function, with exponentially decaying tail in the direction of extreme, converges asymptotically to Gumbel model (*e.g.*, normal, log-normal, Rayleigh random variables), similarly, if the tails of the density function decay as a polynomial, then the extremes converge to the Frechet distribution (*e.g.*, Cauchy random variable), and finally, if the tail is limited in the direction of the extremes, then the limiting extreme value distribution would be of the Weibull type (*e.g.*, uniformly distributed random variable).

Efforts have also been made in recent years to generalize the classical extreme value theory to consider situations when the random variables do not form iid sequences. The works of Gumbel (1958), Galambos (1978), Leadbetter *et al.*, (1983), Castillo (1988), Kotz and Nadarajah (2000), and Coles (2001) provide extensive accounts of the relevant studies.

The book by Leadbetter *et al.*, (1983) documents the progress in extending the classical extreme value theory to the cases of dependent random variable and stationary sequences and continuous parameter processes for the case of Gaussian random processes. The book unifies these two developments and provides a general account on the theory of extremes from which the known results for stationary normal sequences and processes are

obtained as special cases.

The book by Castillo (1988) considers the situation when the knowledge of common PDF is lacking, but instead the analyst has access to only sample of observations. The theorems that enable the identification of basin of attraction to which a given random variable belongs to, cannot be used in this context. Consequently, alternate set of tools for the determination of domains of attraction of the parent distribution from observed samples are needed. Before we proceed to discuss the possible manner in which this problem could be handled, it is important to emphasize the relevance of this problem to time variant reliability analysis of randomly excited vibrating systems:

1. In the context of structural reliability analysis, one needs to often deal with nonlinear dynamical systems responding to Gaussian/non-Gaussian random excitations. The response processes are often non-Gaussian in nature. The theory of extremes of non-Gaussian random processes over specified duration is not well developed.
2. Analysis of reliability of nonlinear structural system to random excitations using Monte Carlo simulations pose serious computational difficulties, especially if the probability of failure is of the order of  $10^{-5}$  or even less. This is all the more true for large scale systems in which solution for a single sample problem could itself be time consuming.

The problem could be tackled by using Monte Carlo simulations with in-built variance reduction capabilities. In recent years, the use of mathematical theorems on change of probability measure based on Girsanov theorem and the results from stochastic control theory, have been explored to deal with this problem (Macke and Bucher 2003, Olsen and Naess 2006). This line of work is not yet fully explored in the context of time variant reliability of structural dynamical systems. We propose in this study an alternative strategy that has potential to lead to estimation of probability of structural failure with relatively less number of samples than what is needed for a brute

force Monte Carlo simulation technique. The strategy consists of simulating limited number of time histories of the system response process, and making an objective choice of the appropriate extreme value distribution based on this data. Once the choice is made, the parameters of the limiting form of the extreme value distribution can be estimated using a reasonably small sample size. Following this, estimates on probability of failure, even when the probability is small, could be made. The present study explores this possibility and presents a procedure for achieving this.

### 3 Selection of limiting distribution of extremes based on limited data

The problem of identifying the asymptotic form of the distribution of the extremes of the outcome of a sequence of random variables based on limited observations of the underlying random phenomena lies at the heart of the study of extremes of environmental processes. The limitations on the extent of the available data in this context are natural, given the constraints on the availability of the past recorded data. In the context of structural reliability of time varying systems we could artificially enforce the restriction that the asymptotic form of the extreme value distribution be established based on limited simulation data. If this is considered acceptable, we could treat the problem of reliability assessment using the same methods as are used in the study of limited data resulting from observations of environmental processes. Following Castillo (1988) and Hasofer and Wang (1992), we consider three alternative methods to deal with this problem: one is due to the work of Pickands (1975), the next is due to Galambos (1980, as cited in the book by Castillo 1988), and the third is due to Hasofer and Wang (1992). A brief description of these methods is provided in the following subsections.

#### 3.1 Pickands III method

We begin by considering a random variable  $X$  with PDF  $F(x)$ . According to Pickands (1975), the assumption that  $F(x)$  lies in the domain of attraction of an extreme value distribution is equiv-

alent to the statement

$$\begin{aligned} & \lim_{u \rightarrow \omega(F)} P[X > x + u | X > u] \\ &= \frac{F(u+x)}{1-F(u)} = \left(1 + \frac{cx}{a}\right)^{-1/c} \\ & a > 0; \quad -\infty < c < \infty; \quad 1 + \frac{cx}{a} \geq 0 \end{aligned} \quad (3)$$

where  $u$  is an event in the event space  $\omega(F)$ , and  $c$  and  $a$  are parameters of the distribution. For  $c = 0$ , the right hand side is given in a limiting sense, as

$$\lim_{u \rightarrow \omega(F)} P[X > x + u | X > u] = \exp\left(-\frac{x}{a}\right), \quad (4)$$

where for  $c > 0$ ,  $c < 0$ , and  $c = 0$ ,  $F(x)$  lies in the domain of attraction for maxima of the Frechet, Weibull, and Gumbel distributions, respectively. Equation 3 shows that the conditional PDF  $G(x)$  of  $X - u$ , given  $X \geq u$  for  $u$  large enough, is approximately of the form

$$G(x) = 1 - \left(1 + \frac{cx}{a}\right)^{-1/c} \quad (5)$$

This fact allows the estimation of  $c$  from a sample. Based on the estimated value, a decision on the domain of attraction could be made. Let  $X_{(1)}, X_{(2)}, \dots, X_{(n)}$  denote the descending order statistics of a sample size  $n$ . For  $s = 1, 2, \dots, [n/4]$ , where  $[x]$  refers to the integer part of  $x$ , we compute

$$d_s = \max_x |F_s(x) - G_s(x)| \quad (6)$$

where  $F_s(x)$  is the empirical distribution of  $X - X_{(4s)}$ , given that  $X \geq X_{(4s)}$ , and  $G_s(x)$  is the distribution as given in equation 5 with  $a$  and  $c$  replaced by the estimators

$$c = \frac{\log\left(\frac{(X_{(s)} - X_{(2s)})}{(X_{(2s)} - X_{(4s)})}\right)}{\log(2)} \quad (7a)$$

$$a = \frac{c(X_{(2s)} - X_{(4s)})}{2^c - 1} \quad (7b)$$

We choose  $M$  to be the smallest integer solution of the equation

$$d_M = \min_{1 \leq s \leq \lfloor \frac{n}{4} \rfloor} d_s \quad (8)$$

Table 1: Sampling distribution of  $c$  for a sample size of 100 to be used in Pickands' method

| CDF | 0.01   | 0.02   | 0.05   | 0.10   | 0.20   | 0.30   | 0.50   | 0.70   | 0.80  | 0.90  | 0.95  | 0.98  | 0.99  |
|-----|--------|--------|--------|--------|--------|--------|--------|--------|-------|-------|-------|-------|-------|
| $c$ | -0.520 | -0.452 | -0.404 | -0.340 | -0.260 | -0.209 | -0.112 | -0.038 | 0.156 | 0.330 | 0.544 | 0.760 | 0.916 |

and take the values of  $c$  and  $a$  as those associated with  $s = M$  in equations 7a and 7b. It has been shown by Pickands that the estimation of tail probabilities of  $F_s(x)$  by  $G_s(x)$  leads to consistent estimates. Based on the estimate of  $c$  as obtained above, a decision on the domain of attraction could be made. Castillo (1988) has considered the problem of determination of significance levels for testing the hypothesis that  $F(x)$  belongs to a Gumbel-type domain of attraction rather than a Weibull or Frechet type, based on simulation studies on the PDF of parameter  $c$ . This allows approximating the critical values of  $c$  for selected values of type I error probability, or approximate significance level to be obtained. The PDF of estimate of  $c$  determined for a sample size of 100 is reproduced in Table 1.

### 3.2 Galambos method

This method tests if a given  $F(x)$  belongs to the basin of attraction of Gumbel distribution for the largest values. This is based on the result that the random variable

$$Z = \frac{X - u}{E[X - u | X > u]} \quad (9)$$

is unit exponential. That is,

$$\lim_{u \rightarrow \omega(F)} \frac{P[X > x + u | X > u]}{E[X - u | X > u]} = \exp(-x) \quad (10)$$

Thus to test if a given sample of  $X$  emanates from a random variable which belongs to the basin of attraction of Gumbel PDF or not, we adopt the following steps:

- (a) Choose a number  $u$  (Galambos 1987).
- (b) Select those  $X_j$  from the sample that exceed  $u$ .
- (c) For each  $X_j > u$ , compute the transformed

value

$$Y_j = \frac{X_j - u}{E[X_j - u | X_j > u]} = \frac{X_j - u}{\sum_{X_j > u} ((X_j - u) / m(u))} \quad (11)$$

where  $m(u)$  is the number of  $X_j$  which exceed  $u$ .

- (d) Employ Kolmogorov Smirnov test to test the hypothesis that  $Y_j$  follows a unit exponential law. This involves the formation of the test statistic

$$\max_y |F_{m(u)}(y) - 1 + \exp(-y)| \quad (12)$$

where  $F_{m(u)}(y)$  is the empirical PDF associated with the exceedances of the level  $u$  in the sample. In order to calculate the significance level, we must take into account that the mean value of the exponential law was estimated from the sample by using equation 11. The book by Castillo (1988) provides the tables [originally due to Lillefors (1969)] to facilitate this.

### 3.3 Hasofer-Wang hypothesis test

Consider  $x(t)$  to be a realization of a stationary random process. The null hypothesis here is the statement that the domain of attraction of the data on extremes is the Gumbel probability distribution. The following are the steps in the Hasofer-Wang hypothesis test (Hasofer and Wang 1992)

1. Determine the number of extremes ( $N$ ) in the given sample  $x(t)$  corresponding to time duration  $T$ . Arrange the extremes in descending order  $x_{1:N} \geq x_{2:N} \geq \dots \geq x_{N:N}$ .
2. Select the top  $k$  values  $x_{1:N} \geq x_{2:N} \geq \dots \geq x_{k:N}$  with  $k = 1.5\sqrt{N}$ , and determine the test statistic  $\tilde{W}$  using the following formula

$$\tilde{W} = \frac{k(\bar{X} - X_{k:N})^2}{(k-1) \left[ \sum_{i=1}^k (X_{i:N} - \bar{X})^2 \right]},$$

$$\text{where } \bar{X} = \frac{\left( \sum_{i=1}^k X_{i:N} \right)}{k} \quad (13)$$

3. The value of the test statistic  $W = 10^4 \tilde{W}$  is compared with the upper and lower percentage points ( $W \lim_U$  and  $W \lim_L$ ) given in Table 2 for different significance levels.
4. The domain of attraction is ascertained to be Gumbel or Weibull or Frechet as follows:
  - a.  $W > W \lim_U$  : accept the hypothesis that the data belongs to the domain of attraction of Weibull distribution.
  - b.  $W_U > W > W_L$  : accept the null hypothesis that the data belongs to the domain of attraction of Gumbel distribution.
  - c.  $W < W \lim_L$  : accept the hypothesis that the data belongs to the domain of attraction of Frechet distribution.

The papers by Dunne and Ghanbari (2001) and Alves and Neves (2006) contain discussions on the details of the Hasofer-Wang test.

## 4 Stochastic dynamical systems

### 4.1 Identification of basin of attraction based on data

Attention in this study is focused on the extremes of response of a dynamical system driven by white Gaussian noise or by filtered white noise. The governing equations could be written in the form

$$dx(t) = a[x(t), t]dt + b[x(t), t]dw(t),$$

$$\text{for } x(t_0) = x_0 \quad (14)$$

Here  $x(t)$ ,  $x_0$  and  $a[x(t), t]$  are  $d \times 1$  vectors,  $b[x(t), t]$  is a  $d \times m$  matrix and  $dw(t)$  is a  $m \times 1$  vector of increments of the standard Brownian motion process. The problem on hand consists of determining the probability

$$\lim_{t_I \rightarrow \infty} P[x_k(t) < \alpha_k \forall t \in (t_I, t_I + T)]$$

$$= \lim_{t_I \rightarrow \infty} P \left[ \max_{t \in (t_I, t_I + T)} x_k(t) < \alpha_k \right]$$

$$= P[x_{k \max} < \alpha_k] \quad (15)$$

in the time interval  $(t_I, t_I + T)$ , where  $x_{k \max} = \lim_{t_I \rightarrow \infty} \max_{t \in (t_I, t_I + T)} x_k(t)$  and  $\alpha_k$  is the threshold below which the response is considered. The steps to evaluate the above probability are as follows:

- (a) Simulate  $N$  samples of  $\{x_{ki}(t)\}_{i=1}^N$  over the interval  $(t_I, t_I + T)$  with  $t_I \rightarrow \infty$  using Monte Carlo simulation technique.
- (b) Assemble all the extremes in  $\{x_{ki}(t)\}_{i=1}^N$  into a single array  $\theta$ . The size of this array would vary from one simulation run to the other.
- (c) Apply the Pickands, Galambos and (or) Hasofer-Wang test to decide upon the asymptotic form of the extreme value distribution to whose basin of attraction the data  $\theta$  belongs to.
- (d) Simulate  $\tilde{N}$  samples of  $\{x_{ki}(t)\}_{i=1}^{\tilde{N}}$  and determine  $x_{kmi} = \max_{t \in (t_I, t_I + T)} x_{ki}(t); i = 1, \dots, \tilde{N}$ .
- (e) Estimate parameters of PDF of  $x_{km}$  identified in step (c) above.
- (f) Estimate the required probability  $P[x_{k \max} < \alpha_k]$  using this PDF.

It is expected that  $N \ll \tilde{N}$ . Also  $\tilde{N}$  itself is large enough to provide estimate of parameters of the extreme value distribution, and does not depend upon the value of  $P[x_{k \max} < \alpha_k]$ . This implies that  $P[x_{k \max} < \alpha_k]$  could be evaluated with relatively small sample size than what is typically required in a brute force Monte Carlo simulation strategy.

### 4.2 Simulation of samples of system response

To implement the steps outlined in the previous subsection, we need to simulate sample solutions of equation 14. The method for numerical solution of this type of equations differs significantly from that of ordinary differential equations due

Table 2: Upper and lower percentage points for  $W$  in the Hasofer-Wang test.

| Sample size | Percentage level          |       |       |       |                           |        |        |        |
|-------------|---------------------------|-------|-------|-------|---------------------------|--------|--------|--------|
|             | Lower tail ( $W \lim_L$ ) |       |       |       | Upper tail ( $W \lim_U$ ) |        |        |        |
|             | 0.01                      | 0.025 | 0.05  | 0.10  | 0.10                      | 0.05   | 0.025  | 0.01   |
| 13          | 333.8                     | 395.6 | 457.7 | 538.4 | 1599.5                    | 1827.5 | 1998.5 | 2204.6 |
| 14          | 305.6                     | 361.2 | 416.3 | 489.6 | 1406.3                    | 1589.4 | 1749.6 | 1934.4 |
| 15          | 288.1                     | 339.4 | 389.3 | 456.5 | 1275.6                    | 1450.4 | 1596.2 | 1768.1 |
| 16          | 272.8                     | 321.3 | 368.8 | 431.5 | 1183.3                    | 1334.9 | 1469.4 | 1629.5 |
| 17          | 258.6                     | 306.0 | 349.6 | 407.7 | 1095.0                    | 1234.7 | 1357.9 | 1508.3 |
| 18          | 247.4                     | 290.2 | 332.0 | 386.5 | 1017.1                    | 1143.9 | 1259.7 | 1397.7 |
| 19          | 237.1                     | 277.6 | 316.6 | 368.5 | 950.4                     | 1064.5 | 1171.1 | 1301.4 |
| 20          | 226.9                     | 265.4 | 302.5 | 350.7 | 888.8                     | 997.3  | 1096.5 | 1220.9 |
| 21          | 217.7                     | 255.0 | 289.1 | 333.6 | 836.0                     | 938.1  | 1027.2 | 1145.8 |
| 22          | 210.1                     | 244.9 | 278.3 | 321.0 | 787.3                     | 881.9  | 968.7  | 1077.2 |
| 25          | 189.4                     | 219.3 | 248.8 | 285.4 | 672.1                     | 747.4  | 821.1  | 910.8  |
| 30          | 165.0                     | 189.2 | 212.6 | 241.7 | 535.5                     | 593.6  | 650.7  | 719.9  |
| 40          | 131.7                     | 149.5 | 166.1 | 186.4 | 377.1                     | 413.6  | 451.5  | 497.0  |
| 50          | 110.4                     | 124.1 | 136.6 | 151.8 | 289.5                     | 316.5  | 340.2  | 371.1  |
| 60          | 96.4                      | 106.9 | 116.6 | 128.8 | 232.9                     | 253.8  | 270.8  | 293.3  |
| 80          | 76.5                      | 84.2  | 91.0  | 98.9  | 168.4                     | 179.9  | 190.7  | 205.5  |
| 100         | 63.6                      | 69.2  | 74.3  | 80.2  | 129.6                     | 138.4  | 146.4  | 155.5  |
| 200         | 35.4                      | 37.6  | 39.9  | 41.9  | 59.4                      | 62.2   | 64.8   | 68.1   |
| 500         | 16.3                      | 16.9  | 17.4  | 18.0  | 22.6                      | 23.2   | 23.8   | 24.5   |

to the peculiar nature of the underlying calculus. These aspects have been discussed in literature. The book by Kloeden and Platen (1995) provides a comprehensive account of the development of numerical methods for solution of initial value problems as in equation 14. In our study we employ the order 1.5 strong Taylor scheme as outlined by Kloeden and Platen (1995). We consider the time discretization of equation 14 with  $0 = t_0 < t_1 < \dots < t_N = T$  in the time interval  $[0, T]$ . Furthermore, we take the time steps to be uniform with  $\Delta = T/N$ . The discretization scheme is given by (Kloeden and Platen 1995)

$$\begin{aligned}
 Y_k(n+1) &= Y_k(n) + a_k(n)\Delta + b_k(n)\Delta W \\
 &+ \frac{1}{2}L^1 b_k(n) \left\{ (\Delta W)^2 - \Delta \right\} \\
 &+ L^1 a_k(n)\Delta Z + L^0 b_k(n) \{ \Delta W \Delta - \Delta Z \} \\
 &+ \frac{1}{2}L^0 a_k(n)\Delta^2 \\
 &+ \frac{1}{2}L^1 L^1 b_k(n) \left\{ \frac{1}{3}(\Delta W)^2 - \Delta \right\} \Delta W
 \end{aligned}$$

(16)

for  $n = 0, 1, 2, \dots, N - 1$  and  $k = 1, 2, \dots, d$  with  $Y_0 = x_0$ . In the above equation

$$\begin{aligned}
 L^0 &= \frac{\partial}{\partial t} + \sum_{k=1}^d a_k \frac{\partial}{\partial x_k} + \frac{1}{2} \sum_{k=1}^d \sum_{l=1}^d b_k b_l \frac{\partial^2}{\partial x_k \partial x_l} \\
 L^1 &= \sum_{k=1}^d b_k \frac{\partial}{\partial x_k}
 \end{aligned}$$

(17)

and  $\Delta W$  and  $\Delta Z$  are normal random variables given by

$$\begin{Bmatrix} \Delta W \\ \Delta Z \end{Bmatrix} = \begin{bmatrix} \sqrt{\Delta} & 0 \\ 0.5\Delta^{1.5} & \frac{0.5\Delta^{1.5}}{\sqrt{3}} \end{bmatrix} \begin{Bmatrix} U_1 \\ U_2 \end{Bmatrix}$$

(18)

where  $U_1$  and  $U_2$  being the standard normal random variables having the properties

$$\begin{Bmatrix} U_1 \\ U_2 \end{Bmatrix} \equiv N \left( \begin{Bmatrix} 0 \\ 0 \end{Bmatrix}, \begin{bmatrix} 1 & 0 \\ 0 & 1 \end{bmatrix} \right)$$

(19)



### 4.3 Out-crossing rate based on solution of Fokker-Planck-Kolmogorov equation

The  $d$ -dimensional transition probability density function  $p(x, t | x_0, t_0)$  associated with solutions of equation 14 is known to satisfy the Kolmogorov forward and backward equations. The forward equation, also known as the Fokker-Planck-Kolmogorov (FPK) equation, is given by

$$\frac{\partial p(x, t | x_0, t_0)}{\partial t} = - \sum_{j=1}^d \frac{\partial}{\partial x_j} [a_j(x, t) p(x, t | x_0, t_0)] + \frac{1}{2} \sum_{i=1}^d \sum_{j=1}^d \frac{\partial^2}{\partial x_i \partial x_j} [(b \Xi b^t) p(x, t | x_0, t_0)] \quad (20)$$

Here  $\Xi$  is the covariance matrix of the driving noise process vector. When a steady state is possible it turns out that  $\frac{\partial p(x, t | x_0, t_0)}{\partial t} = 0$ , and consequently the governing equation is given by

$$- \sum_{j=1}^d \frac{\partial}{\partial x_j} [a_j(x, t) p(x, t)] + \frac{1}{2} \sum_{i=1}^d \sum_{j=1}^d \frac{\partial^2}{\partial x_i \partial x_j} [(b \Xi b^t) p(x, t)] = 0 \quad (21)$$

This reduced form of the FPK equation is exactly solvable for a class of problems. This class includes a class of nonlinear oscillators with a single degree of freedom, and the governing equations are of the form

$$\ddot{y} + \beta \dot{y} + f(y) = w(t) \quad (22)$$

where  $\beta$  is a system parameter,  $f(y)$  is a function of system response  $y$  and  $w(t)$  is a stationary random process with  $\langle w(t) \rangle = 0$  and  $\langle w(t_1)w(t_2) \rangle = 2\pi \Phi \delta(t_1 - t_2)$ . Here  $\Phi$  is the constant of the spectral density of  $w(t)$ ,  $\langle \bullet \rangle$  denotes the mathematical expectation operator and  $\delta(\bullet)$  is the Dirac delta function. In the steady state it can be shown that

$$p(y, \dot{y}) = C \exp \left[ - \frac{\beta}{\pi \Phi} \left\{ \frac{\dot{y}^2}{2} + \int_0^y f(s) ds \right\} \right] \quad (23)$$

where  $C$  is the normalization constant to be chosen such that  $\int_{-\infty}^{\infty} \int_{-\infty}^{\infty} p(y, \dot{y}) dy d\dot{y} = 1$ . It is of interest to note that  $y(t)$  and  $\dot{y}(t)$  are stochastically

independent so that  $p(y, \dot{y}) = p_Y(y) p_{\dot{Y}}(\dot{y})$ . Table 3 provides details of this pdf for a few choices of  $f(y)$  lim.

Once the knowledge of  $p(y, \dot{y})$  is available, one can compute the average rate of up-crossing of a specified level  $\alpha$  using the Rice's formulation:

$$v^+(\alpha) = \int_{-\infty}^{\infty} \int_{-\infty}^{\infty} |\dot{y}| \delta[y - \alpha] p(y, \dot{y}) dy d\dot{y} \quad (24)$$

For the problem on hand, this reduces to

$$v^+(\alpha) = p_Y(\alpha) \int_{-\infty}^{\infty} p_{\dot{Y}}(\dot{y}) d\dot{y} = p_Y(\alpha) \frac{\sigma_{\dot{Y}}^2}{\sqrt{2\pi}} \quad (25)$$

Table 3 provides details of this out-crossing rate as well. Assuming that level  $\alpha$  is high and that the number of crossings of level  $\alpha$  in the duration  $(t_0, t_0 + T)$  with  $t_0 \rightarrow \infty$  could be modeled as a Poisson random variable, a model for the extreme  $Y_m = \max_{t_0 \rightarrow \infty}^{(t_0, t_0 + T)} y(t)$  is obtained as

$$P_{Y_m}(\alpha) = \exp[-v^+(\alpha)T] \quad (26)$$

In the numerical studies we compare the models for extremes from the proposed approach with the analytical models as given by equation 26.

## 5 Numerical examples

In this section, the proposed method is demonstrated for dynamical systems subjected to external random excitation (white Gaussian noise)  $f(t)$  of zero mean and constant standard deviation  $\sigma$ . In this section  $\eta$  is used to denote the damping coefficient and  $\omega$  for the natural frequency of the system.

### 5.1 Linear SDOF systems

We begin by considering the response of an sdof system with white Gaussian noise excitation given by

$$\ddot{x} + 2\eta\omega\dot{x} + \omega^2x = f(t) \quad (27)$$

$$\text{for } x(0) = x_0, \dot{x}(0) = \dot{x}_0$$

$$\text{and } \langle f(t_1)f(t_2) \rangle = \sigma^2\delta(t_1 - t_2)$$

Table 3: Properties of steady state solutions of sdof systems considered in section 4.3

|               |   |   |  |
|---------------|---|---|--|
|               | $f(y) = \omega^2; \beta = 2\eta\omega$  | $f(y) = \omega^2(y + \epsilon y^3)$   | $f(y) = \frac{2\omega^2 d}{\pi} \tan\left\{\frac{\pi y}{2d}\right\}; -d < y < d$<br>$\beta = 2\alpha$  |
| $p(y)$        | $\frac{1}{\sqrt{2\pi}\sigma_{y_0}} \exp\left[-\frac{y^2}{2\sigma_{y_0}^2}\right]$<br>$\sigma_{y_0}^2 = \frac{\pi\Phi}{\beta\omega^2}$                 | $\frac{1}{\sqrt{2\pi}Q(\rho)\sigma_{y_0}} \exp\left[-\frac{1}{\sigma_{y_0}^2}\left(\frac{y^2}{2} + \frac{\rho y^4}{4\sigma_{y_0}^2}\right)\right]$<br>$Q(\rho) = \frac{1}{\sqrt{2\pi}\sigma_{y_0}} \int_{-\infty}^{\infty} \exp\left[-\frac{1}{\sigma_{y_0}^2}\left(\frac{y^2}{2} + \frac{\rho y^4}{4\sigma_{y_0}^2}\right)\right] dy$<br>$\rho = \epsilon\sigma_{y_0}^2; \sigma_{y_0}^2 = \frac{\pi\Phi}{\beta\omega^2}$ | $\frac{\sqrt{\pi}}{2d} \frac{\Gamma\left(\frac{n}{2}+1\right)}{\Gamma\left(\frac{n+1}{2}\right)} \left\{\cos\left(\frac{\pi y}{2d}\right)\right\}^n; n \geq 0$<br>$n = \frac{4d^2}{\pi\sigma_0^2}; \sigma_0^2 = \frac{\pi\Phi}{2\alpha\omega^2}$ |
| $p(\dot{y})$  | $\frac{1}{\sqrt{2\pi}\sigma_{\dot{y}_0}} \exp\left[-\frac{\dot{y}^2}{2\sigma_{\dot{y}_0}^2}\right]$<br>$\sigma_{\dot{y}_0}^2 = \frac{\pi\Phi}{\beta}$ | $\frac{1}{\sqrt{2\pi}\sigma_{\dot{y}_0}} \exp\left[-\frac{\dot{y}^2}{2\sigma_{\dot{y}_0}^2}\right]$<br>$\sigma_{\dot{y}_0}^2 = \frac{\pi\Phi}{\beta}$   | $\frac{1}{\sqrt{2\pi}\sigma_0\omega} \exp\left[-\frac{\dot{y}^2}{2\sigma_0^2\omega^2}\right]$  |
| $v^+(\alpha)$ | $\frac{\sigma_{y_0}}{\sqrt{2\pi}} \frac{1}{\sqrt{2\pi}\sigma_{y_0}} \exp\left[-\frac{\alpha^2}{2\sigma_{y_0}^2}\right]$                               | $\frac{\sigma_{y_0}}{\sqrt{2\pi}} \frac{1}{\sqrt{2\pi}Q(\rho)\sigma_{y_0}} \exp\left[-\frac{1}{\sigma_{y_0}^2}\left(\frac{\alpha^2}{2} + \frac{\rho\alpha^4}{4\sigma_{y_0}^2}\right)\right]$  | $\frac{\sigma_0\omega}{\sqrt{2\pi}} \frac{\sqrt{\pi}}{2d} \frac{\Gamma\left(\frac{n}{2}+1\right)}{\Gamma\left(\frac{n+1}{2}\right)} \left\{\cos\left(\frac{\pi\alpha}{2d}\right)\right\};  \alpha  \leq d$                                       |

This equation can be recast into the Ito stochastic differential equation form as

$$\begin{aligned} dx_1 &= x_2 dt \\ dx_2 &= \{-\omega^2 x_1 - 2\eta\omega x_2\} dt + \sigma dw(t) \end{aligned} \quad (28)$$

For the purpose of numerical simulation of the solution path we use the discretization given in equations 16-19.

$$\begin{aligned} Y_1(k+1) &= Y_1(k) + a_1(k)\Delta + L^1 a_1(k)\Delta Z \\ &\quad + \frac{1}{2} L^0 a_1(k)\Delta^2 \\ Y_2(k+1) &= Y_2(k) + a_2(k)\Delta + b_2(k)\Delta W \\ &\quad + L^1 a_2(k)\Delta Z + \frac{1}{2} L^0 a_2(k)\Delta^2 \\ a_1(k) &= Y_2(k); \\ a_2(k) &= -[2\eta\omega Y_2(k) + \omega^2 Y_1(k)]; \\ b_2(k) &= \sigma; \\ L^0 a_1(k) &= a_2(k); \\ L^0 a_2(k) &= a_1(k)(-\omega^2) + a_2(k)(-2\eta\omega); \\ L^1 a_1(k) &= \sigma; \\ L^1 a_2(k) &= \sigma(-2\eta\omega) \end{aligned} \quad (29)$$

In the numerical work we take  $\eta = 0.08, \lim \omega = 2\pi \text{rad/s}, \sigma = 1.0$  and  $T = 35\text{s}$ . Figures 1(a) and

1(b) show, respectively, the estimates of time histories of the standard deviation of the displacement and velocity processes obtained using 5000 samples of Monte Carlo simulations. The exact solutions in the steady state are also shown in this figure. Figure 1(c) compares the PDF of displacement response obtained using simulations with the exact solution. From these figures, it is evident that the simulation algorithm employed in the study works satisfactorily. Figure 1(d) shows a typical time history of the sample displacement process along with the extremes that have been identified computationally. The results on the Galambos test (with 245 samples and  $u = 0.1374$ ) for identifying the domain of attraction for extremes are shown in figures 1(e) and 1(f). The Pickands method yielded with 100 samples a value of  $c = 1.2662$ . Similarly, with  $N = 245$  and  $k = 23$ , the W statistic in the Hasofer-Wang test was obtained as 320.0. From these results we can conclude that at 5% significance level the data can be taken to belong to the domain of attraction of Gumbel distribution for the extremes (see Table 2). Accordingly, the parameters of the Gumbel PDF were estimated using 100 samples and an estimate for the PDF of extremes was obtained. Figure 1(g) shows this PDF along with the estimates

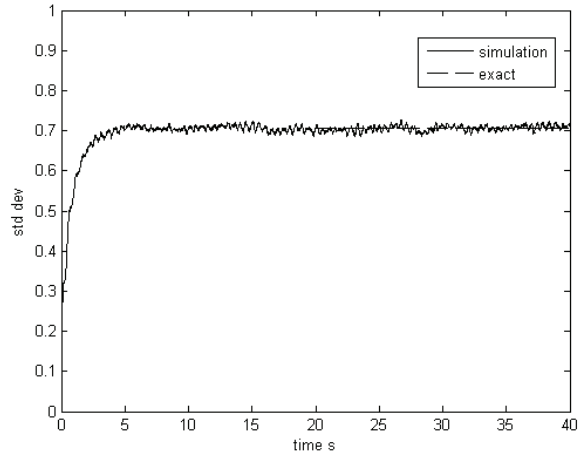


Fig. 1 (a)

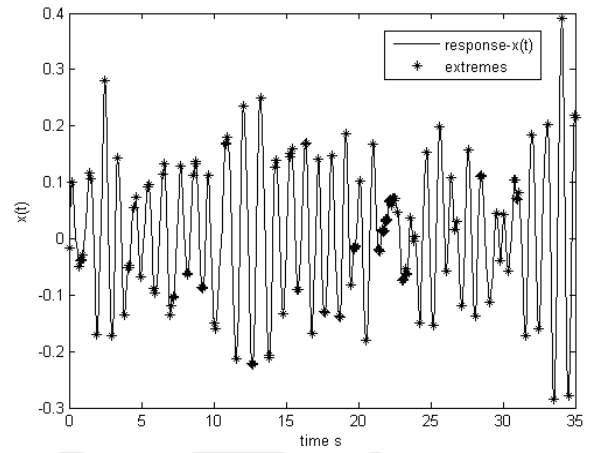


Fig. 1 (d)

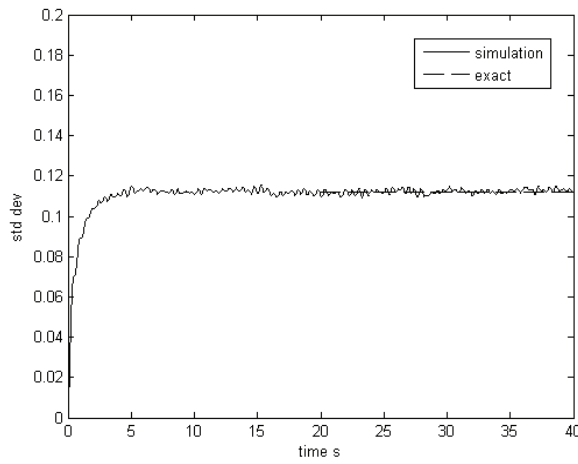


Fig. 1 (b)

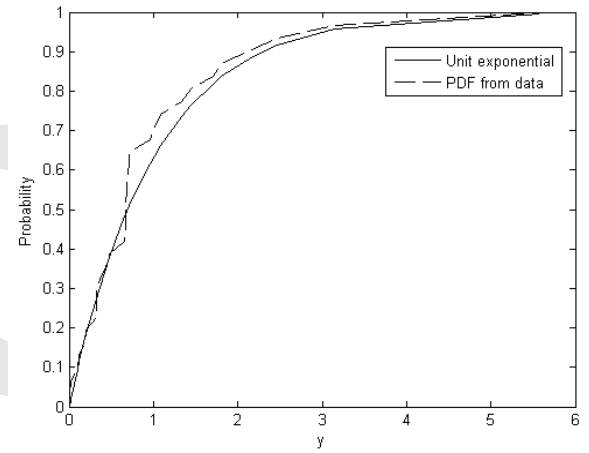


Fig. 1 (e)

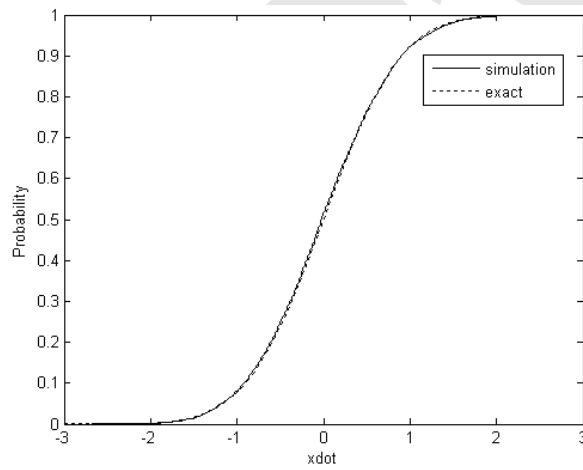


Fig. 1 (c)

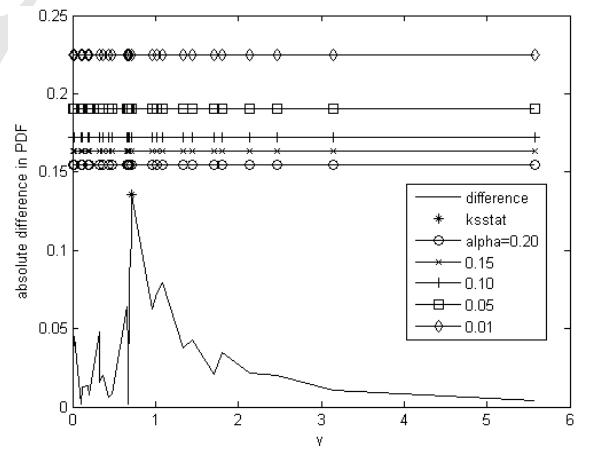


Fig. 1 (f)

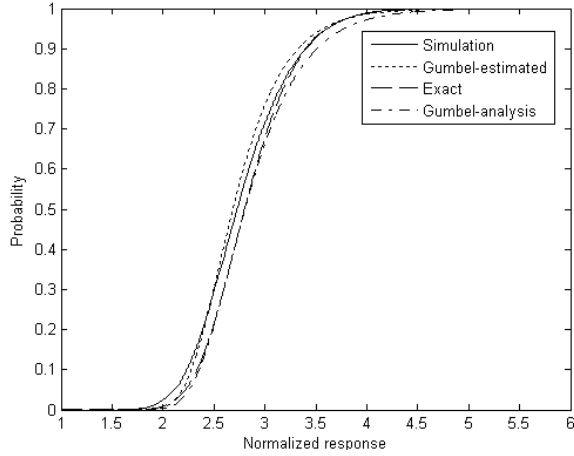


Fig. 1 (g)

Figure 1: Linear sdf system under white noise excitations;  $\eta = 0.08$ ;  $\omega = 2\pi\text{rad/s}$ ; (a) standard deviation of displacement; (b) standard deviation of velocity; (c) PDF of displacement; (d) sample time histories with extremes marked; (e) unit exponential and the empirical PDF; (f) results of the K-S test ( $u = 0.1374$ , sample size = 245); (g) PDF models for extremes.

obtained using a 5000 sample simulation and analytical predictions on extremes using equation 26. In this case it is noted that the analytical PDF for extremes has the form

$$P_{X_m}(\alpha) = \exp \left[ -\frac{\sigma_{\dot{x}} T}{2\pi\sigma_x} \exp \left\{ -\frac{\alpha^2}{2\sigma_x^2} \right\} \right] \quad (30)$$

where  $\alpha$  is the response threshold,  $T$  is the time duration of interest and  $\sigma_{\dot{x}}$  and  $\sigma_x$  are the standard deviations of the response processes  $\dot{x}$  and  $x$ , respectively. In figure 1(g) the results according to the above equation are termed as “exact/analytical”. It may be noted that this PDF is not in the Gumbel form. Introducing the notations

$$\zeta = \frac{\alpha}{\sigma_x} \quad \text{and} \quad N_x^+(0) = \frac{\sigma_{\dot{x}}}{2\pi\sigma_x} \quad (31)$$

we write

$$\exp(-\alpha) = N_x^+(0) T \exp \left( -\frac{\zeta^2}{2} \right) \quad (32)$$

From this it follows

$$\zeta = [2\alpha + 2\ln \{N_x^+(0)T\}]^{\frac{1}{2}}. \quad (33)$$

By expanding the right hand side of equation 33 in Taylor’s expansion and retaining only the first two terms, we get

$$\zeta \cong [2\ln \{N_x^+(0)T\}]^{\frac{1}{2}} + \frac{\alpha}{[2\ln \{N_x^+(0)T\}]^{\frac{1}{2}}} \quad (34)$$

Using the notation  $C_1 = [2\ln \{N_x^+(0)T\}]^{1/2}$ , we can write  $\alpha = C_1(\zeta - C_1)$ . Then we obtain

$$P_{X_m}(\alpha) = \exp \left[ -\exp \left\{ -C_1 \left( \frac{\alpha}{\sigma_x} - C_1 \right) \right\} \right] \quad (35)$$

This form of the PDF conforms to the Gumbel form. In figure 1(g) the results from this model are designated as “Gumbel-analysis”.

From figure 1(g) it can be observed that the PDF for the extremes obtained using the procedure proposed in this work compares well with the simulation results than with the analytical predictions based on equations 30 and 35.

## 5.2 Duffing-Van der Pol’s oscillator

Here we consider oscillators governed by equations of the form

$$\ddot{x} + 2\eta\omega\dot{x} - v\dot{x}(1 - 4x^2) + \omega^2x + \mu x^3 = f(t)$$

$$\text{for } x(0) = x_0, \dot{x}(0) = \dot{x}_0$$

$$\text{and } \langle f(t_1)f(t_2) \rangle = \sigma^2\delta(t_1 - t_2) \quad (36)$$

where  $v$  and  $\mu$  are system parameters. In the numerical work we take  $\omega = 2\pi\text{rad/s}$ ,  $\eta = 0.08$ ,  $v = 0.1$ ,  $\mu = 50$  and  $\sigma = 1.0$ . The above equation can be recast in a form compatible with equation 14 as

$$\begin{aligned} dx_1(t) &= x_2 dt \\ dx_2(t) &= \left\{ -2\eta\omega x_2 + v x_2(1 - 4x_1^2) - \omega^2 x_1 \right. \\ &\quad \left. - \mu x_1^3 \right\} dt + \sigma dw(t) \end{aligned} \quad (37)$$

Thus we get

$$d = 2, \quad m = 1,$$

$$a_1 = x_2$$

$$a_2 = -2\eta\omega x_2 + v x_2(1 - 4x_1^2) - \omega^2 x_1 - \mu x_1^3$$

$$b_1 = 0; \quad b_2 = \sigma$$

(38)

which, in conjunction with the discretization scheme outlined in equations 16-19, lead to the discrete set of equations that are used in the Monte Carlo simulations.

We first consider the case of Duffing oscillator (i.e., equation 38 with  $\nu = 0$ ). Analytical models for the system response based on the exact solution of the governing FPK equation in the steady state are summarized in Table 3 (Refer to equation 22 in section 4.3). Figures 2(a) and (b) show the results of the Galambos test ( $u = 1.0943$ ; sample size = 235). The Pickands test with 100 samples lead to a value of  $c = -1.1214$ . The Hasofer-Wang statistic  $W$  was obtained as 511.1 ( $N = 235, k = 23$ ), which again confirms Gumbel basin of attraction (at 5% significance level, Table 2). This leads to the conclusion that the data belongs to the Gumbel's basin of attraction for the extremes. The results on PDF of extremes over 35s using 5000 sample simulations and a Gumbel model, whose parameters are estimated using 100 samples, are shown in figure 2(c).

We next consider the case of Van der Pol's oscillator (i.e., equation 38 with  $\mu = 0$ ). This oscillator is characterized by the presence of one stable limit cycle with the origin being unstable. Furthermore, the oscillator does not belong to the class of systems for which the exact steady state solution for the governing FPK equation is obtainable. Figure 3(a) shows a sample realization of the response vector in the form of a phase-plane plot. The trajectory originates from rest, and the limit cycle action forces the trajectory towards the stable limit cycle. In figures 3(b) and 3(c) the PDFs of the displacement and velocity (normalized with respect to their standard deviations) are superimposed on the PDF of standard normal random variable. The departure from normality in the response is evident in these figures displaying the well known bimodal character. Results from the Galambos test ( $u = 0.6355$  sample size = 581) are shown in figures 3(d) and 3(e). This leads to the conclusion that, at 5% significance level, the hypothesis that the data belongs to the domain of attraction of Gumbel for extremes should be accepted. On the other hand, the Pickands test with 100 sam-

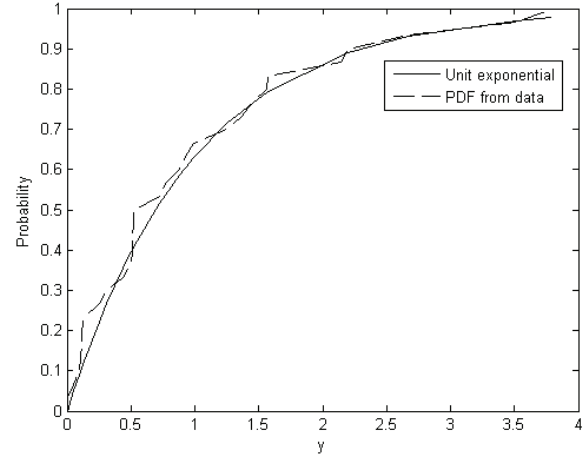


Fig. 2 (a)

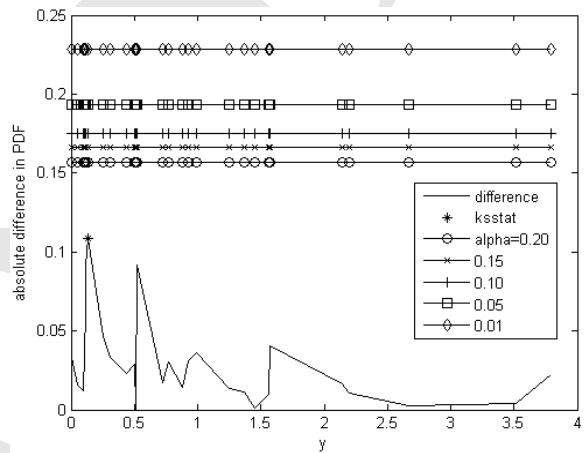


Fig. 2 (b)

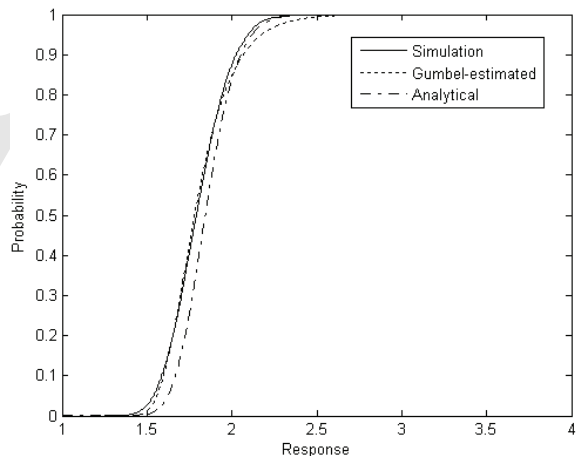


Fig. 2 (c)

Figure 2: The Duffing sdof system under white noise excitations;  $\eta = 0.08$ ;  $\omega = 2\pi$  rad/s;  $\mu = 50$ ; (a) unit exponential and the empirical PDF; (b) results of the K-S test ( $u = 1.0943$ , sample size = 235); (c) PDF models for extremes.

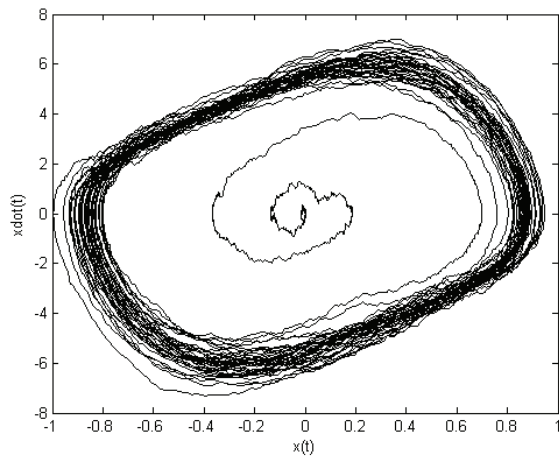


Fig. 3 (a)

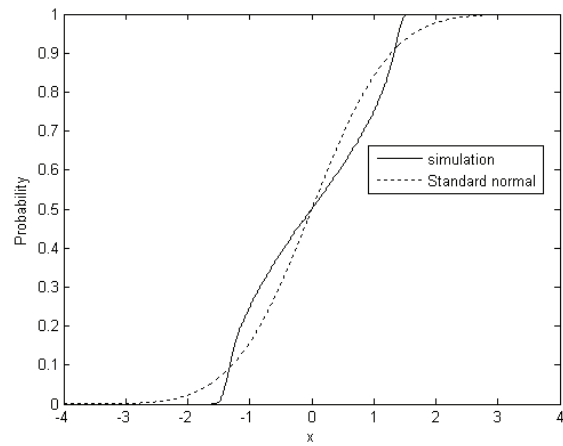


Fig. 3 (b)

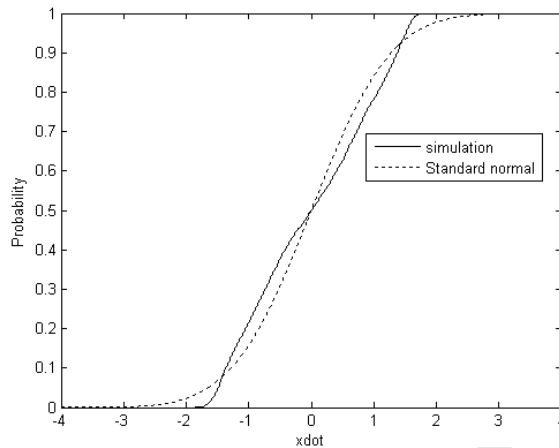


Fig. 3 (c)

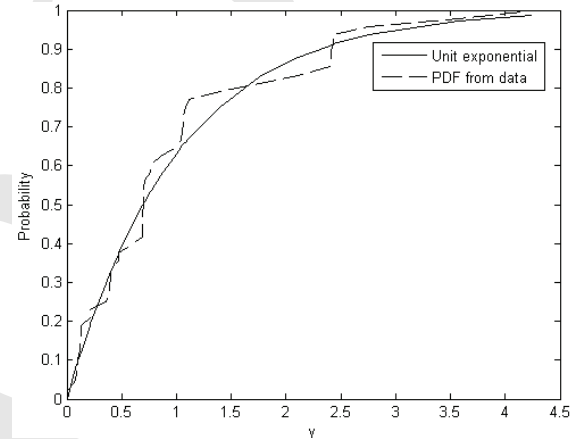


Fig. 3 (d)

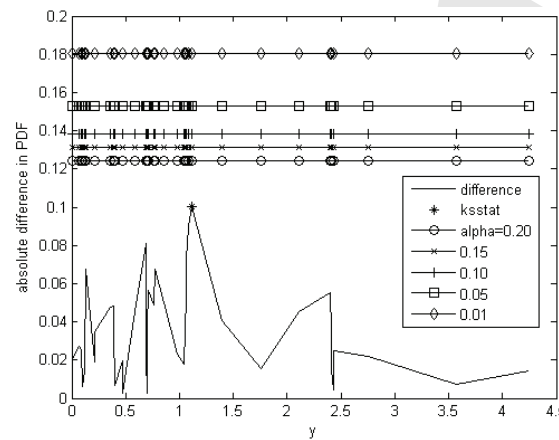


Fig. 3 (e)

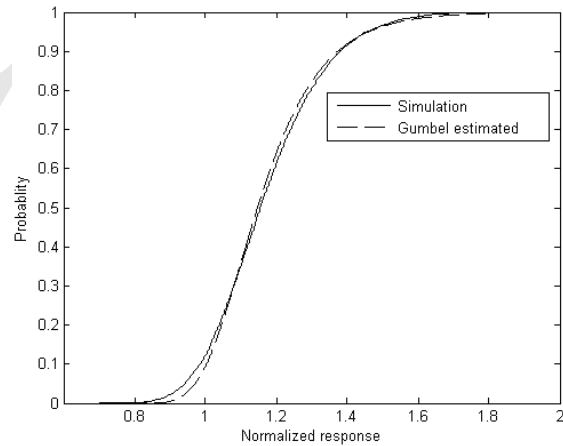


Fig. 3 (f)

Figure 3: The Van Der Pol sdf system under white noise excitations;  $\eta = 0.08$ ;  $\omega = 2\pi$  rad/s;  $\nu = 0.10$ ; (a) Phase-plane plot; (b) PDF of displacement process; (c) PDF of velocity process; (d) unit exponential and the empirical PDF; (e) results of the K-S test ( $u = 0.6355$ , sample size = 581); (f) PDF models for extremes.

ples lead to the estimate of  $c = -0.4677$ . This leads to the rejection of the hypothesis (at 5% significance level) that the data belongs to the domain of attraction of Gumbel. In this case the Galambos and Pickands tests lead to contradictory conclusions. Similar conclusion is also reached from the Hasofer-Wang test in which  $W = 259.6$  ( $N = 581$ ,  $k = 36$ ) is obtained. Figure 3(f) compares the empirical PDF for extremes with 5000 samples along with a Gumbel model, whose parameters are estimated using 100 samples. Figures 4(a)-(e) show results of the Galambos test on data from Duffing-Van der Pol oscillator for different combinations of parameters  $\mu$  and  $\nu$ . The results presented are of particular interest, since the Galambos test indicates that the data belongs to the domain of attraction of Gumbel extreme value distribution, while the Pickands' test reveals the opposite. It may be noted that the value of  $c$  with 100 samples as per Pickands' method is provided in the caption to the figures 4(a)-(e).

### 5.3 Tangent stiffness system

Here we consider systems governed by equations of the form

$$\ddot{x} + 2\eta\dot{x} + \frac{2d\omega^2}{\pi} \tan\left(\frac{\pi x}{2d}\right) = f(t)$$

for  $x(0) = x_0$ ,  $\dot{x}(0) = \dot{x}_0$   
and  $\langle f(t) \rangle = 0$ ;  $\langle f(t_1)f(t_2) \rangle = \sigma^2\delta(t_1 - t_2)$

(39)

This type of oscillator has been studied earlier by Klein (1964), and exact solutions for the steady system response have been obtained from the governing FPK equations (see Table 3). The stiffness characteristics of this system ensures that the displacement process remains bounded between  $(-d, d)$ . Consequently, Gumbel models for extremes can be expected to be invalid for this class of systems.

For the purpose of conducting Monte Carlo simulations we discretize the above governing equation using the algorithm outlined in equations 16-19. For this purpose we write equation 39 in the

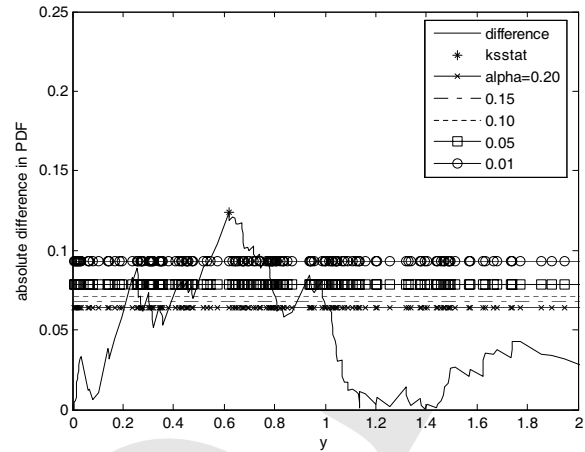


Fig. 4 (a)  $\mu = 50$ ,  $\nu = 0.1$  Pickands,  $c = -0.2542$  (100 samples)

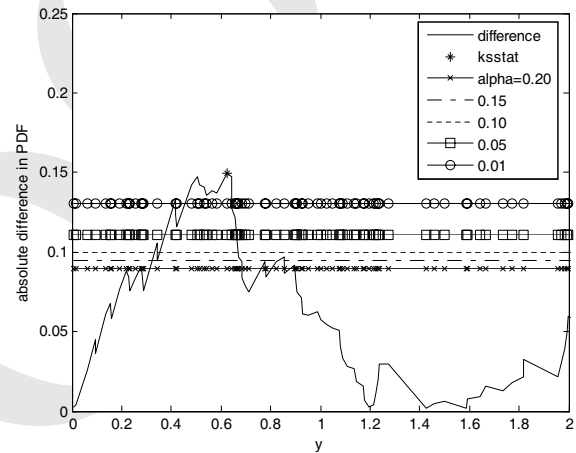


Fig. 4 (b)  $\mu = 100$ ,  $\nu = 0.0$  Pickands'  $c = -0.1871$  (100 samples)

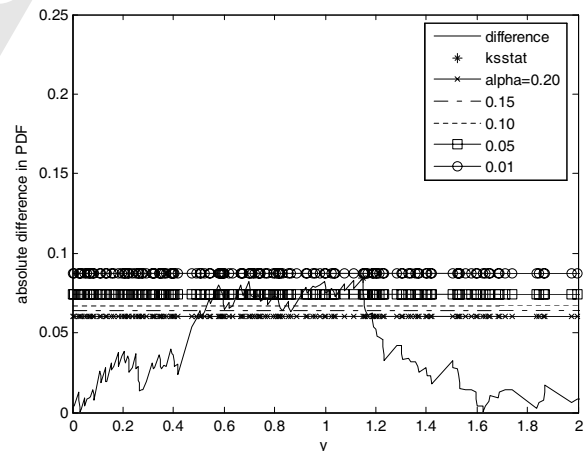


Fig. 4 (c)  $\mu = 100$ ,  $\nu = 0.2$  Pickands'  $c = -0.1189$  (100 samples)

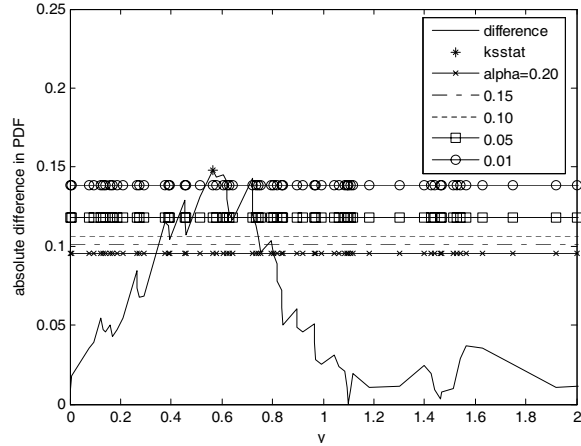


Fig. 4 (d)  $\mu = 100$ ,  $v = 0.5$  Pickands'  $c = -0.1293$  (100 samples)

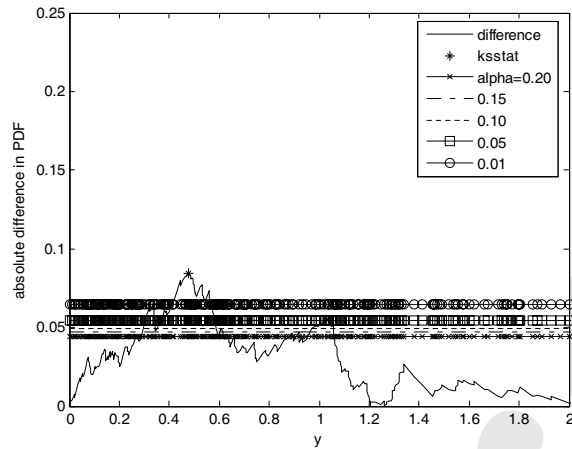


Fig. 4 (e)  $\mu = 100$ ,  $v = 4.0$  Pickands'  $c = -0.1212$  (100 samples)

Figure 4: Results of the Galambos test and Pickands test for the Duffing-Van Der Pol oscillator.

form

$$\begin{aligned} dx_1(t) &= x_2 dt \\ dx_2(t) &= \left( -2\eta x_2 - \frac{2d\omega^2}{\pi} \tan \left\{ \frac{\pi x_1}{2d} \right\} \right) dt + \sigma dw(t) \end{aligned} \quad (40)$$

By comparing equation 40 with equation 14 we

get

$$\begin{aligned} a_1 &= x_2 \\ a_2 &= -2\eta x_2 - \frac{2d\omega^2}{\pi} \tan \left\{ \frac{\pi x_1}{2d} \right\} \end{aligned} \quad (41)$$

$$b_1 = 0$$

$$b_2 = \sigma$$

We use the notations

$$\sigma_0^2 = \frac{\pi S}{2\eta\omega^2}, \quad \sigma^2 = 2\pi S, \quad \text{and} \quad n = \frac{4d^2}{\pi^2\sigma_0^2} \quad (42)$$

In the numerical study we take  $S = 0.0040$ ,  $T = 30s$ ,  $t_0 = 5s$ ,  $\omega = 10\text{rad/s}$ , and  $\eta = 0.05\omega$ . The values of  $n$  are 1, 2, and 5. Samples of the response vector plotted in the form of phase-plane plots are shown in figures 5(a), 5(b) and 5(c) for  $n = 5, 2$ , and 1, respectively. The analytical results on the first order probability density function of  $x(t)$  in the steady state are depicted in figures 5(d), 5(e), and 5(f) for  $n = 5, 2$  and 1, respectively. It is to be noted that, for a given value of excitation intensity, smaller values of  $n$  implies smaller values for the bounding parameter  $d$ . This feature is reflected in the response characteristics as can be evidenced from the shape of phase-plane plots (figures 5 (a)-(c)) and the probability density functions (figures 5 (d)-(f)). As has been already noted, the displacement response in this case would be limited between  $(-d, d)$ . The results of Galambos test for  $n = 5, 2$  and 1 are shown in figures 5(g), 5(h), 5(i), 5(j), 5(k), and 5(l), respectively. The Pickands test with 100 samples revealed the value of  $c$  to be  $-0.2635, -0.4502$  and  $-1.0800$ , respectively. Based on the Galambos test it can be concluded that for  $n = 5$  and 2, Gumbel model for the extremes could be used, while for  $n = 1$ , the Weibull model is obtained. According to the results from the Pickands test (at 5% significance level), the Gumbel model for extremes is acceptable for  $n = 5$  (figure 5(m)) and not acceptable for  $n = 1$ . For the case of  $n = 2$ , one could conclude that either the Gumbel or Weibull model could be used.

#### 5.4 Hysteretic oscillator (Bouc's oscillator)

In this example we consider randomly driven nonlinear systems in which the force of resistance



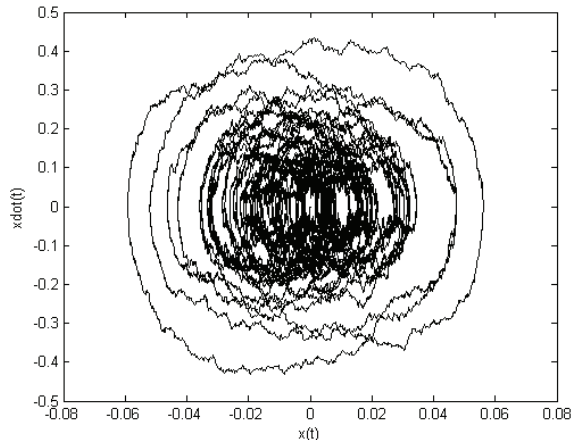


Fig. 5 (a)

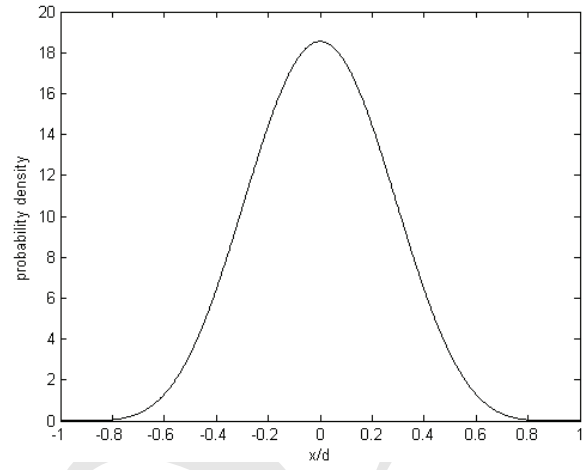


Fig. 5 (d)

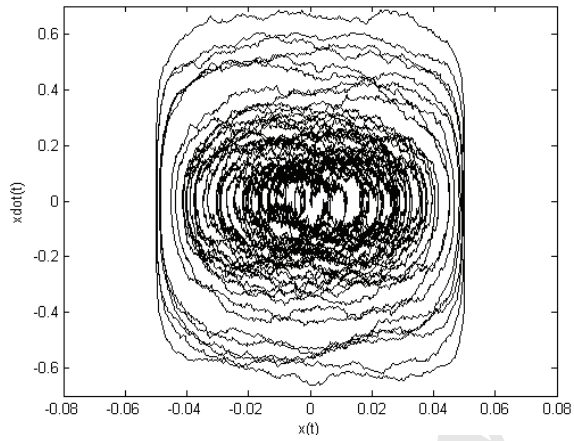


Fig. 5 (b)

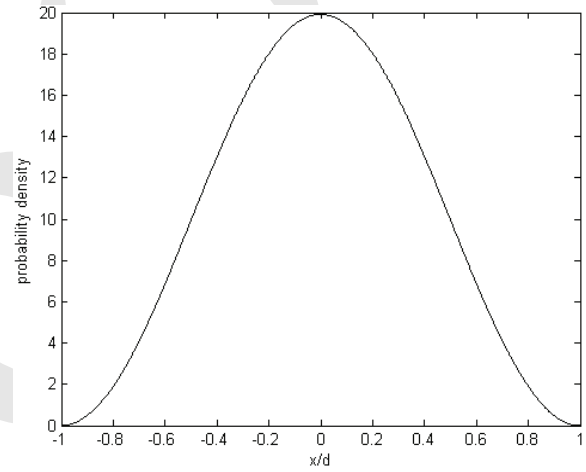


Fig. 5 (e)

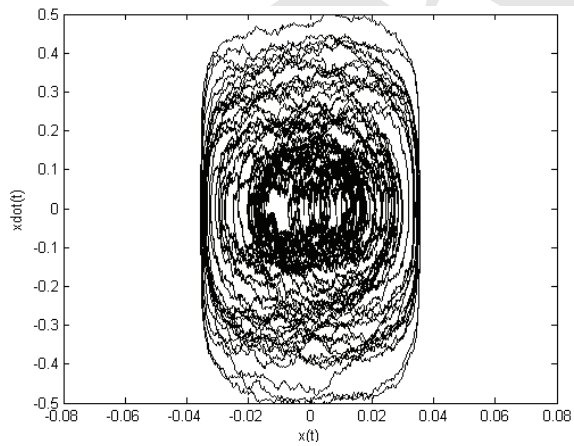


Fig. 5 (c)

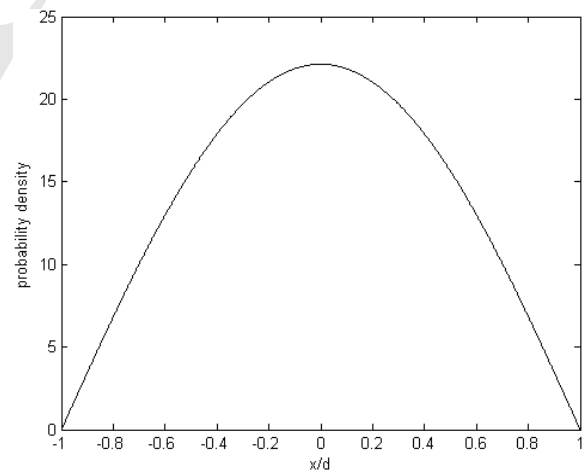


Fig. 5 (f)

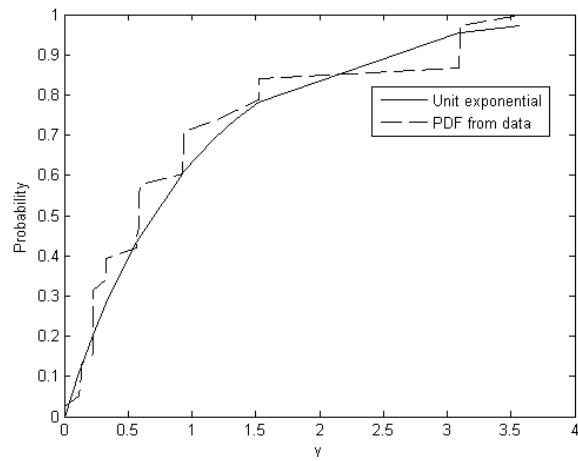


Fig. 5 (g)

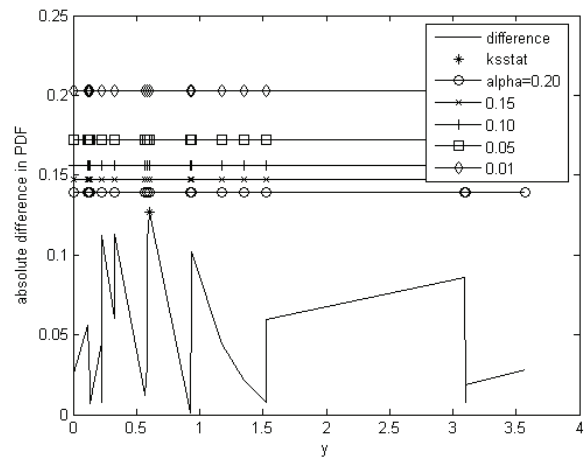


Fig. 5 (j)

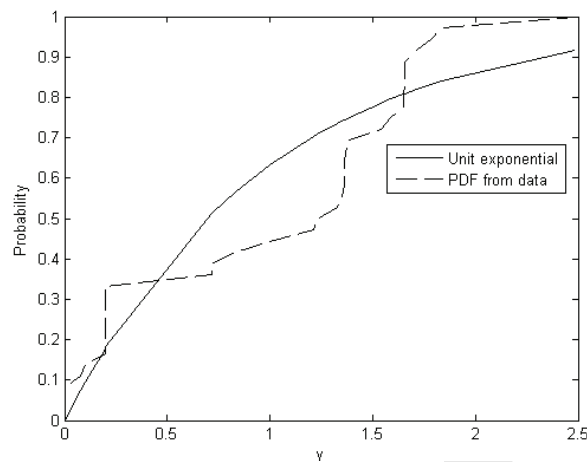


Fig. 5 (h)

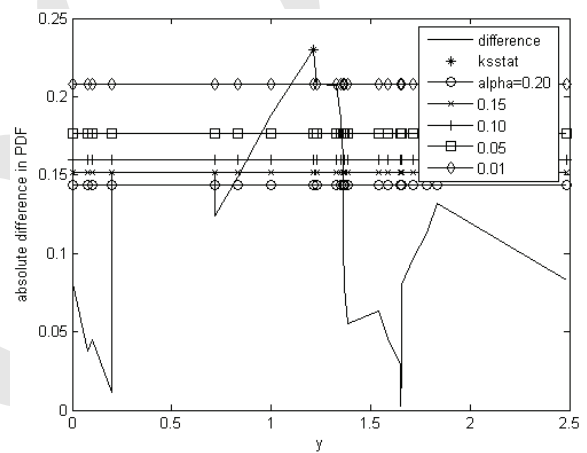


Fig. 5 (k)

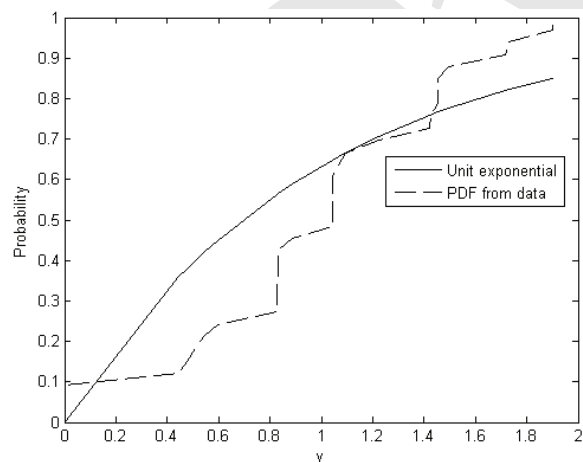


Fig. 5 (i)

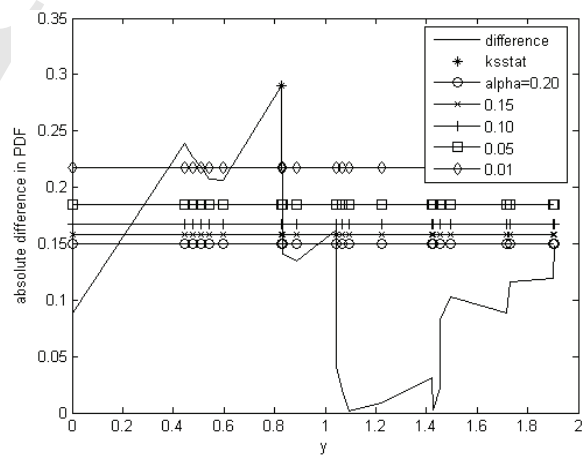


Fig. 5 (l)

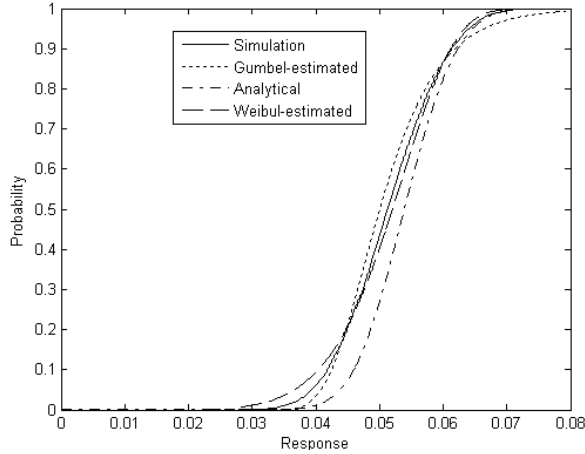


Fig. 5 (m)

Figure 5: The tangent stiffness sdof system under white noise excitations;  $\omega = 10$  rad/s;  $\eta = 0.05\omega$ ;  $S = 0.0040$  (a) Phase-plane plot for  $n=5$ ; (b) Phase-plane plot for  $n=2$ ; (c) Phase-plane plot for  $n=1$ ; (d) pdf of displacement for  $n=5$ ; (e) pdf of displacement for  $n=2$ ; (f) pdf of displacement for  $n=1$ ; (g) unit exponential and the empirical PDF  $n=5$ ; (h) unit exponential and the empirical PDF  $n=2$ ; (i) unit exponential and the empirical PDF  $n=1$ ; (j) results of the K-S test  $n=5$ ; (k) results of the K-S test  $n=2$ ; (l) results of the K-S test  $n=1$ ; (m) PDF models for extremes  $n=5$ .

at any time instant is dependent upon the response time history up to that time instant. These types of oscillators are of interest in problems of earthquake engineering in which structures are designed to display controlled inelastic behavior under the action of random earthquake induced loads. A commonly used model for this class of systems, exemplified through a randomly driven sdof system, is given by

$$\begin{aligned} \ddot{x} + 2\eta\omega\dot{x} + \lambda x + (1-\lambda)z &= f(t) \\ \dot{z} &= -\gamma|\dot{x}|z|z|^{n-1} - \beta\dot{x}|z|^n + A\dot{x} \\ \text{for } x(0) &= x_0, \dot{x}(0) = \dot{x}_0, z(0) = z_0 \\ \text{and } \langle f(t) \rangle &= 0; \langle f(t_1)f(t_2) \rangle = \sigma^2\delta(t_1 - t_2) \end{aligned} \quad (43)$$

Here by adjusting the values of the model parameters  $\lambda, \gamma, n, \beta$  and  $A$ , different shapes for the hysteresis loops could be generated (Wen 1986).

These problems do not belong to the class of problems for which exact solution to the governing FPK equation is presently possible. We begin by recasting the above equation in the Ito form as

$$\begin{aligned} dx_1(t) &= x_2 dt \\ dx_2(t) &= (-2\eta\omega x_2 - \lambda x_1 - (1-\lambda)x_3) dt + \sigma dw(t) \\ dx_3(t) &= (-\gamma|x_2|x_3|x_3|^{n-1} - \beta x_2|x_3|^n + Ax_2) dt \end{aligned} \quad (44)$$

This equation is in the form of equation 14 with  $d=3, m=1$  and

$$\begin{aligned} a_1 &= x_2 \\ a_2 &= (-2\eta\omega x_2 - \lambda x_1 - (1-\lambda)x_3) \\ a_3 &= (-\gamma|x_2|x_3|x_3|^{n-1} - \beta x_2|x_3|^n + Ax_2) \\ b_1 &= 0; b_2 = \sigma; b_3 = 0 \end{aligned} \quad (45)$$

The equations can now be discretized to obtain equations of the form 16-19. In doing so it may be noted that

$$\begin{aligned} L^1 a_1 &= \sigma \\ L^1 a_2 &= -2\eta\omega\sigma \\ L^1 a_3 &= \sigma \{ -\gamma \text{sgn}(x_2)x_3|x_3|^{n-1} - \beta|x_3|^n + A \} \\ L^0 a_1 &= a_2 \\ L^0 a_2 &= -\lambda a_1 - a_2 2\eta\omega - a_3(1-\lambda) \\ L^0 a_3 &= a_2 \{ -\gamma \text{sgn}(x_2)x_3|x_3|^{n-1} - \beta|x_3|^n + A \} \\ &\quad + a_3 \left\{ -\gamma|x_2||x_3|^{n-1} \right. \\ &\quad \left. - \gamma|x_2|x_3(n-1)|x_3|^{n-2} \text{sgn}(x_3) \right. \\ &\quad \left. - \beta x_2 n|x_3|^{n-1} \right\} \end{aligned} \quad (46)$$

In the numerical work we take  $\eta = 0.05$ ,  $\lambda = 0.05$ ,  $\beta = 0.5$ ,  $\eta\omega = 0.02$ ,  $A = 1$ ,  $n = 2$  and  $\gamma = 0.5$ . The noise intensity is taken to be  $\sigma = 1.0$ , and the maximum over time duration  $T = 35$ s is sought. Figures 6(a)-(c) illustrate the sample response time histories in the form of phase-plane plots. The results of Galambos test (sample size = 759,  $u = 5.5794$ ) are shown in figures 6(d) and (e). The Pickands test with 100 samples leads to  $c = 1.2405$ . The Hasofer-Wang test leads to  $W = 262.2$  ( $N = 759, k = 41$ ), so that the null hypothesis

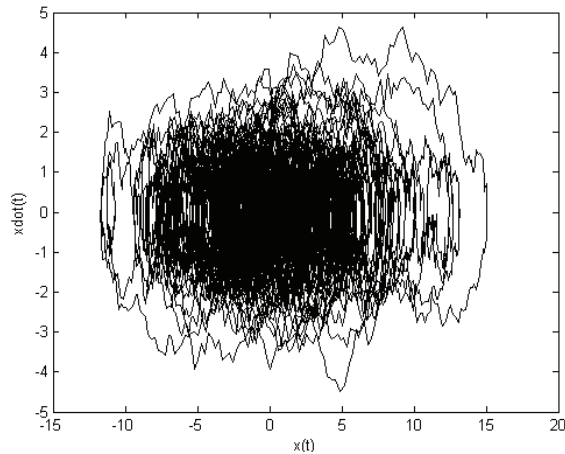


Fig. 6 (a)

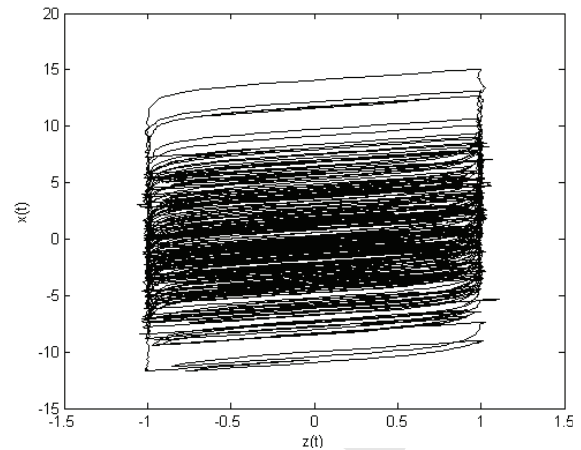


Fig. 6 (b)

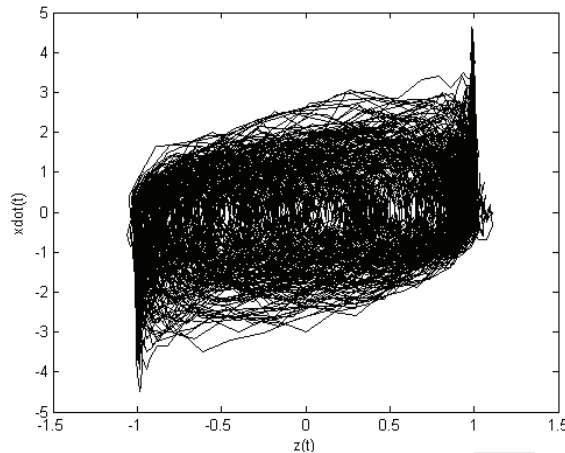


Fig. 6 (c)

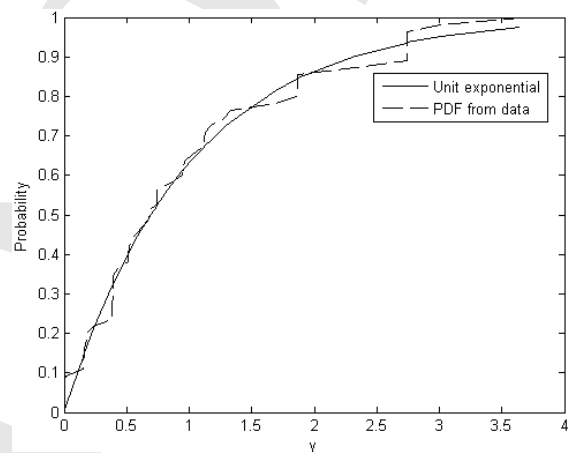


Fig. 6 (d)

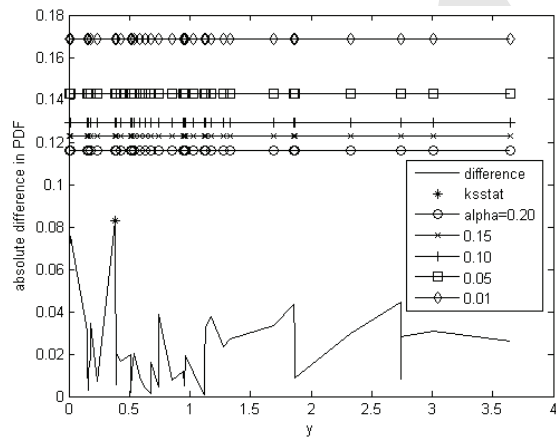


Fig. 6 (e)

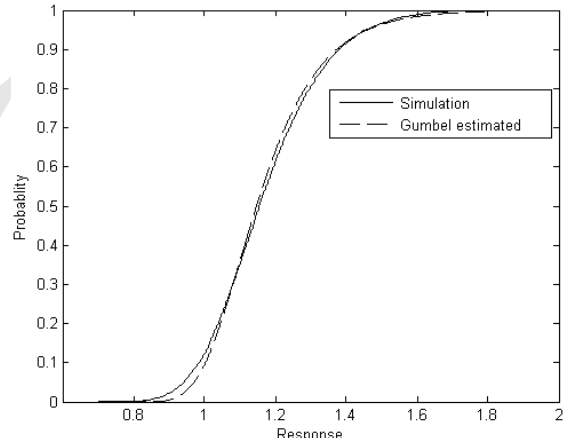


Fig. 6 (f)

Figure 6: The Bouc's oscillator under white noise excitations;  $\eta = 0.05$ ;  $\lambda = 0.05$ ;  $\beta = 0.5$ ;  $\eta\omega = 0.02$ ;  $A = 1$ ;  $n = 2$ ;  $\gamma = 0.5$ ;  $T = 35s$ . (a) Phase-plane plot  $\dot{x}(t)$  versus  $x(t)$ ; (b) Phase-plane plot  $x(t)$  versus  $z(t)$ ; (c) Phase-plane plot  $\dot{x}(t)$  versus  $z(t)$ ; (d) unit exponential and the empirical PDF; (e) results of the K-S test test ( $u = 5.5794$ , sample size = 759); (f) PDF models for extremes.

of the test could be accepted at 5% significance level. Thus the Gumbel model is found to be suitable for modeling the extremes. Figure 6(f) compares the results of 5000 sample simulations on extremes of  $x(t)$  with a prediction from a Gumbel model whose parameters have been estimated using 100 samples. The mutual agreement between these two results is satisfactory.

### 5.5 Nonlinear system with two degrees of freedom

A model with two degrees of freedom with nonlinear stiffness characteristics is governed by the following form of equations of motion

$$\begin{aligned} \ddot{x}_1 + 2\eta_1\omega_1\dot{x}_1 + \alpha_1x_1^3 + \alpha_2x_1^2x_2 + \alpha_3x_1x_2^3 + \alpha_4x_2^3 \\ + \omega_1^2x_1 &= f_1(t) \\ \ddot{x}_2 + 2\eta_2\omega_2\dot{x}_2 + \beta_1x_1^3 + \beta_2x_1^2x_2 + \beta_3x_1x_2^3 + \beta_4x_2^3 \\ + \omega_2^2x_2 &= f_2(t) \end{aligned}$$

for  $x_i(0) = x_{i0}$ ,  $\dot{x}_i(0) = \dot{x}_{i0}$ ;  $i = 1, 2$   
 and  $\langle f_i(t) \rangle = 0$ ,  $\langle f_1(t_1)f_2(t_2) \rangle = 0$ ,  
 $\langle f_i(t_1)f_i(t_2) \rangle = \sigma_i^2\delta(t_1 - t_2)$ ;  $i = 1, 2$

(47)

where  $\eta_i$  ( $i = 1, 2$ ) are the damping coefficients, and  $\alpha_i$  and  $\beta_i$  ( $i = 1, 2, 3, 4$ ) are the system parameters. Expressed in the Ito equation form, the above equations read as

$$\begin{aligned} dy_1(t) &= y_2 dt \\ dy_2(t) &= \left( -2\eta_1\omega_1y_2 - \omega_1^2y_1 - \alpha_1y_1^3 - \alpha_2y_1^2y_3 \right. \\ &\quad \left. - \alpha_3y_1y_3^2 - \alpha_4y_3^3 \right) dt + \sigma_1 dw_1(t) \\ dy_3(t) &= y_4 dt \\ dy_4(t) &= \left( -2\eta_2\omega_2y_4 - \omega_2^2y_3 - \beta_1y_1^3 - \beta_2y_1^2y_3 \right. \\ &\quad \left. - \beta_3y_1y_3^2 - \beta_4y_3^3 \right) dt + \sigma_2 dw_2(t) \end{aligned}$$

(48)

This set of equations is discretized to obtain equations of the form 16-19 which are used in the simulation work. In the numerical work it is assumed that  $\omega_1 = \omega_2 = 2\pi$  rad/s,  $\eta_1 = 0.08$ ,  $\eta_2 = 0.05$ ,  $\alpha_1 = 2$ ,  $\alpha_2 = 4$ ,  $\alpha_3 = 5$ ,  $\alpha_4 = 2.5$ ,  $\beta_1 =$

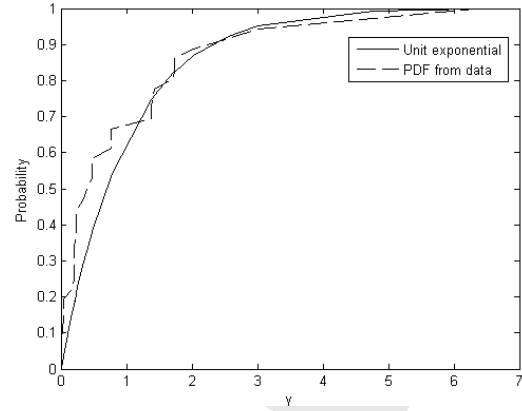


Fig. 7 (a)

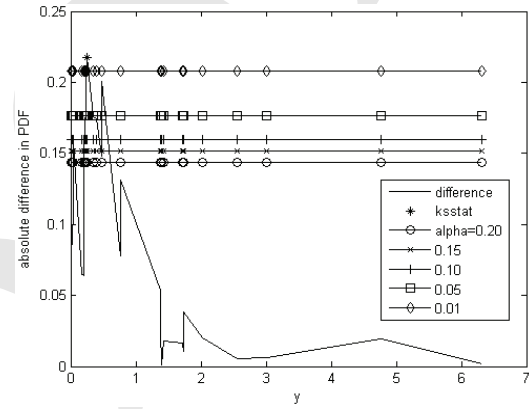


Fig. 7 (b)

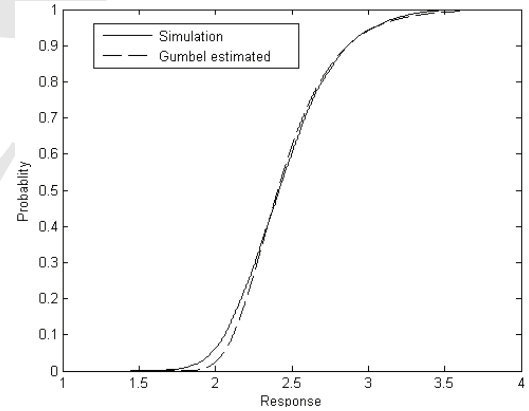


Fig. 7 (c)

Figure 7: The two dof Duffing system under white noise excitations;  $\omega_1 = \omega_2 = 2\pi$  rad/s,  $\eta_1 = 0.08$ ,  $\eta_2 = 0.05$ ,  $\alpha_1 = 2$ ,  $\alpha_2 = 4$ ,  $\alpha_3 = 5$ ,  $\alpha_4 = 2.5$ ,  $\beta_1 = 4$ ,  $\beta_2 = 5$ ,  $\beta_3 = 1.5$ , and  $\beta_4 = 4$ ; (a) unit exponential and the empirical PDF; (b) results of the K-S test ( $u = 1.3106$ , sample size = 335); (c) PDF models for extremes.

Table 4: Geometrical and structural data of the turbine blades considered in Section 5.6

| Radial position<br>(m) | Chord<br>(m) | Relative thickness<br>(%) | Twist<br>(Degrees) | EI flap<br>(MNm <sup>2</sup> ) | EI edge<br>(MNm <sup>2</sup> ) | Mass<br>(kg/m) |
|------------------------|--------------|---------------------------|--------------------|--------------------------------|--------------------------------|----------------|
| 1.46                   | 0.01         | 40.0                      | 0.0                | $1.50 \times 10^{10}$          | $1.50 \times 10^{10}$          | 3000           |
| 2.75                   | 0.01         | 40.0                      | 0.0                | $8.00 \times 10^9$             | $8.00 \times 10^9$             | 1500           |
| 2.96                   | 0.01         | 40.0                      | 0.0                | $2.00 \times 10^9$             | $2.00 \times 10^9$             | 510            |
| 6.46                   | 3.30         | 30.6                      | 8.0                | $5.86 \times 10^8$             | $1.40 \times 10^9$             | 390            |
| 9.46                   | 3.00         | 24.1                      | 7.0                | $2.40 \times 10^8$             | $8.51 \times 10^8$             | 315            |
| 12.46                  | 2.70         | 21.1                      | 6.0                | $1.21 \times 10^8$             | $5.24 \times 10^8$             | 250            |
| 15.46                  | 2.40         | 18.7                      | 5.0                | $6.09 \times 10^7$             | $3.28 \times 10^8$             | 206            |
| 18.46                  | 2.10         | 16.8                      | 4.0                | $3.05 \times 10^7$             | $2.08 \times 10^8$             | 173            |
| 21.46                  | 1.80         | 15.5                      | 3.0                | $1.43 \times 10^7$             | $1.23 \times 10^8$             | 138            |
| 24.46                  | 1.50         | 14.4                      | 2.0                | $5.68 \times 10^6$             | $6.18 \times 10^7$             | 94             |
| 27.46                  | 1.20         | 13.3                      | 1.0                | $1.71 \times 10^5$             | $2.64 \times 10^7$             | 55             |
| 28.96                  | 1.05         | 12.8                      | 0.5                | $7.70 \times 10^5$             | $1.60 \times 10^7$             | 40             |
| 29.86                  | 0.96         | 12.5                      | 0.2                | $4.50 \times 10^5$             | $1.16 \times 10^7$             | 31             |
| 30.56                  | 0.89         | 12.2                      | 0.0                | $2.70 \times 10^5$             | $8.60 \times 10^6$             | 25             |

4,  $\beta_2 = 5$ ,  $\beta_3 = 1.5$  and  $\beta_4 = 4$ . The noise intensities are taken to be  $\sigma_1 = 10$  and  $\sigma_2 = 0$ . Figures 7(a) and (b) show the results of the Galambos test as applied to samples of  $y_1(t)$  with ( $u = 1.3106$  and sample size = 335). The Pickands test with 100 samples yielded  $c = -0.5260$ . The Hasofer-Wang test leads to  $W = 229.4$  ( $N = 335$ ,  $k = 27$ ) for  $y_1(t)$  so that the null hypothesis is accepted at 5% significance level. A Gumbel model was subsequently selected, and figure 7(c) shows the comparison of empirical PDF of extremes with 5000 samples with the Gumbel model whose parameters have been determined using 100 samples.

### 5.6 Reliability of a wind turbine subjected to dynamic wind loads

Here we consider the reliability of a wind turbine structure when it is subjected to dynamic effects of wind loads. This example serves to illustrate the application of the proposed method for reliability analysis when applied to large scale vibration problems. The structure under study consists of a typical 2MW wind turbine with 3 blades with a hub height of 61m and blade diameter of 30m (Figure 8(a)). The values of the other system parameter are summarized in Table 4 (Ahlstrom, 2005). The three-degree tilted rotor produces a blade tip speed of 71m/s while running at a con-

stant speed of 22.3 rotations per minute. The loads induced on the structure in this case are a result of complex fluid-structure interaction. The analysis in the present study is based on the software Flex5 which enables the aeroelastic simulation of wind turbines (Oye 1996). The analysis here involves coupled aerodynamics and structural analysis. Aerodynamic simulation is used for estimation of loads, and the structural analysis is carried out based on modal decomposition and time domain numerical integration. The structural modeling consists of component mode synthesis, in which the tower, turbine blades and the rotor part are modeled as Euler-Bernoulli beams, and the structural matrices for the built-up structure are produced in terms of the modes of the individual substructures in uncoupled states. In the numerical work, the first two modes of the individual substructures are included. This structural model does not include the stiffening effect due to centrifugal forces generated due to blade rotation. The wind velocity is modeled as a sample of stationary Gaussian random field with power spectral density function  $S(f)$  given by the well known Kaimal spectra

$$\frac{fS(f)}{\sigma_1^2} = \frac{(4fL_c/V_{hub})}{(1 + (6fL_c/V_{hub}))^{5/3}} \quad (49)$$

where  $V_{hub}$  is the mean wind speed at hub height averaged over 10min,  $f$  is frequency in Hz,  $\sigma_1$  is the standard deviation of wind velocity component that is obtained by multiplying turbulence intensity (assumed to be 0.41) with the mean wind speed, and  $L_c$  is the integral scale parameter of the velocity component describing the size of the large energy containing eddies in a turbulent flow. A value of 170 is used for  $L_c$  as per IEC specification (IEC 1998). The hub height  $z_{hub}$  in the present example is 61m, and it is assumed that  $V_{hub} = 10\text{m/s}$ . The variation of wind speed along the height of the turbine is taken to be given by  $u(z) = V_{hub} (z/z_{hub})^{0.2}$ , where  $u(z)$  is the velocity of wind at height  $z$  above the ground. The cross-correlation between turbulent fluctuations at points separated in lateral and vertical directions is given by the coherence function

$$coh(r, f) = \exp\left(-8.8\sqrt{\left(\frac{fr}{V_{hub}}\right)^2 + \left(0.12\frac{v}{L_c}\right)^2}\right) \quad (50)$$

Here  $r$  refers to the radial distance of any location from the hub center, and  $v$  is the magnitude of projection of the separation vector between the two points under consideration onto a plane normal to the average wind direction. Wind velocity profile with a mean speed of 10m/s and turbulence intensity of 41% is generated as per the above spectral density function for 10min duration with a time step of 0.08s. Figure 8(b) shows a typical time history of wind velocity. The time histories of the blade tip deflection, bending moment at the blade root and at the tower base, are simulated using the Flex5 software (figures 8(c)-(g)). The following performance functions are considered:

1. The maximum clearance between the blade tip and the tower over a duration of 10min remains less than a prescribed limit (4.5m) (performance function 1).
2. The maximum bending moment at the blade root and at the tower base over a duration of 10min are  $< 3500\text{kNm}$  and  $< 30000\text{kNm}$ , respectively (performance functions 2 and 3).

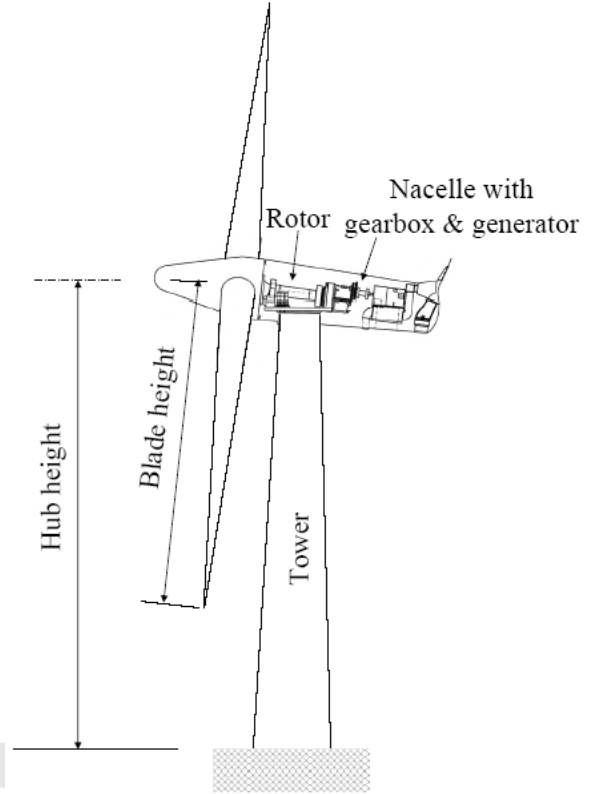


Fig. 8 (a)

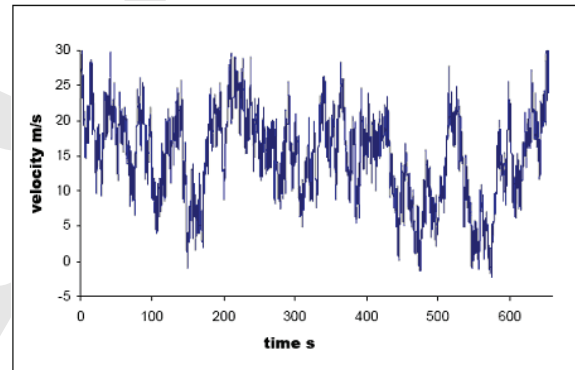


Fig. 8 (b)

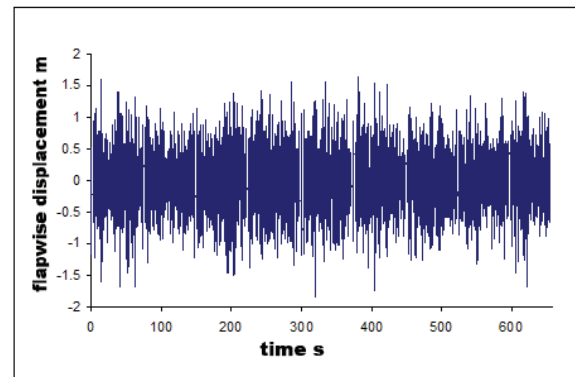


Fig. 8 (c)

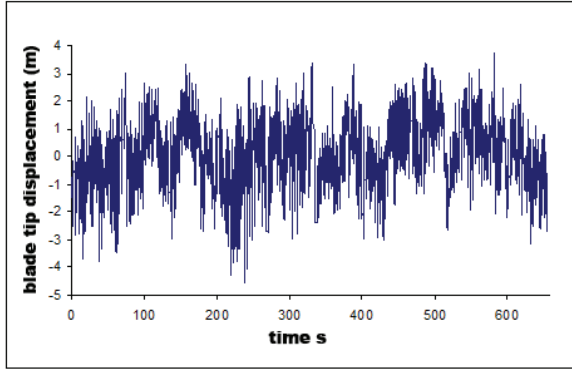


Fig. 8 (d)

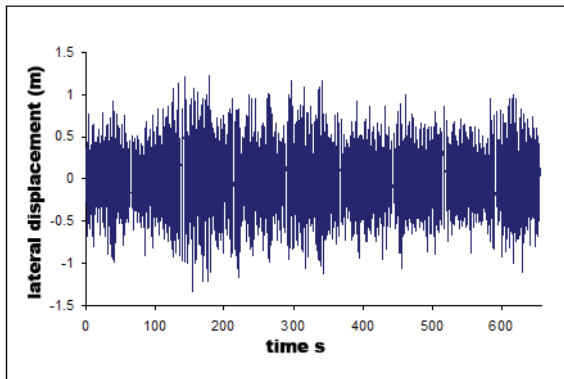


Fig. 8 (e)

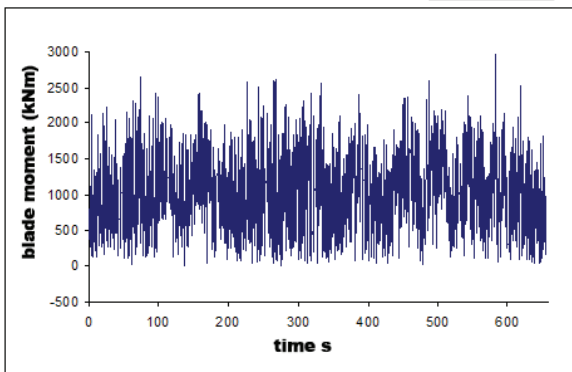


Fig. 8 (f)

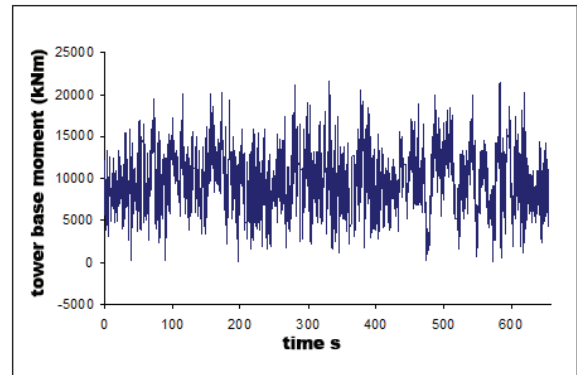


Fig. 8 (g)

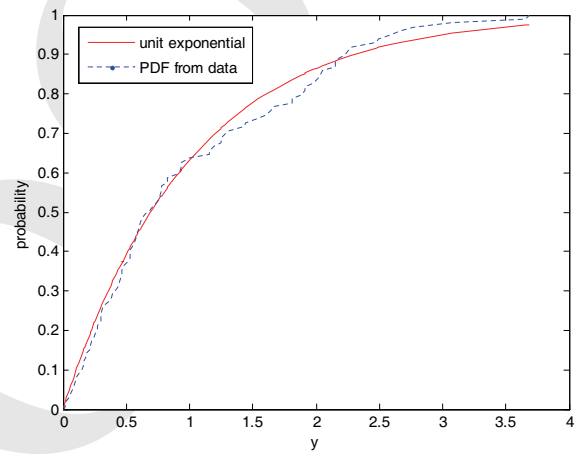


Fig. 8 (h)

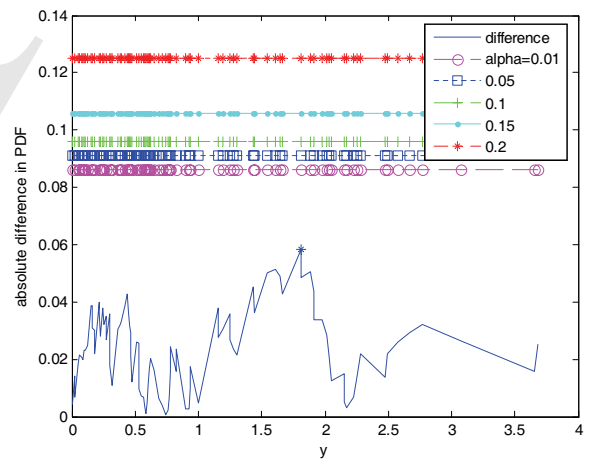


Fig. 8 (i)



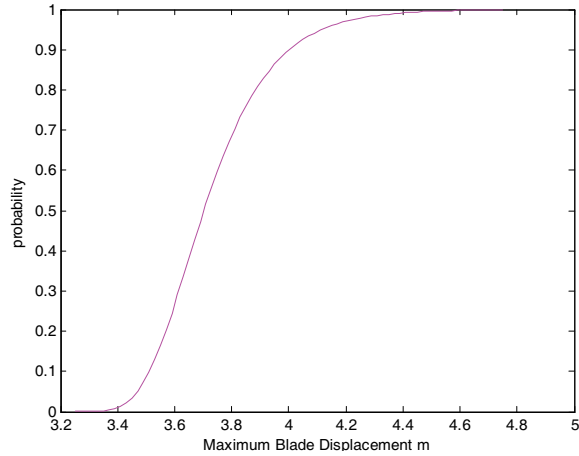


Fig. 8 (j)

Figure 8: Reliability analysis of a wind turbine structure; (a) typical wind turbine structure; flap-wise direction refers to the direction perpendicular to blade chord; edgewise direction is parallel to the blade chord; blade torsion is referred with respect to the axis along the blade length; (b) a sample realization of the velocity of wind at turbine hub shown for a mean wind speed of 10m/s and turbulence intensity of 0.41; (c) flap-wise displacement of the tower top; (d) blade tip deflection; (e) lateral displacement of the tower top; (f) bending moment at blade root; (g) bending moment at tower base; (h) unit exponential and the empirical PDF; (i) results of the K-S test; (j) PDF of the extreme displacement.

3. The maximum lateral and flap-wise tower top acceleration over a duration of 10min is  $< 2\text{m/s}^2$  (performance functions 4 and 5).

The basin of attraction of extremes of each of the response quantities is determined using the Galambos and Pickands tests, and by using peaks contained in 5 samples of the response time histories (each of 10min duration). It is confirmed that the extremes belong to the basin of attraction of Gumbel random variable (figures 8(h) and (i)). Accordingly, further analysis with 100 sample time histories of 10min duration lead to the estimation of the Gumbel parameters for each of the response quantities. Figure 8(j) illustrates the PDF of the response of the extreme blade tip obtained. The probability of failure for the five

performance functions was estimated to be, respectively,  $1.9923\text{e-}004$ ,  $1.3986\text{e-}004$ ,  $2.3359\text{e-}4$ ,  $1.3234\text{e-}006$  and  $2.721\text{e-}003$ . In this example, it is of interest to note that the time required for one sample calculation, including the wind generation and aerodynamic simulation, is about 25mins on a Pentium 2.66GHz 1GB RAM machine. Clearly, a large scale Monte Carlo simulation study for time variant reliability on this type of structures is infeasible, especially to evaluate probability of failure of the order of  $10^{-4}$  and less. It is also to be noted that the analysis outlined here could be carried out even when the time histories as shown in figures 8(c)-(g) are obtained by actual measurements on existing wind turbine structures. This would mean that the procedures for extreme value analysis discussed herein are applicable for studying reliability of existing structures. An example of this class of study is presented in the next section.

### 5.7 Reliability of existing structures

The procedure for identification of the basin of attraction of extremes and subsequent modeling of the PDF of extremes could also be applied when the vibration data emanates from either laboratory or field measurements. To illustrate this possibility we consider the nonlinear system shown in figure 9(a). The system here consists of a cantilever aluminum beam (rectangular cross section of  $19.1 \times 3.1\text{mm}$ ) that is suspended on two steel wires (0.25 mm diameter), and is driven by a band-limited (2-1000 Hz) random dynamic base motion. The wires here are incapable of resisting compressive forces, and consequently the system possesses bilinear stiffness characteristics with the wires contributing to increase in beam stiffness only when they carry tensile forces. An experimental study on this system was conducted by mounting the beam on an electro-dynamic shaker and by measuring the beam acceleration response at a set of four points. The first five natural frequencies of the beam (without wires) estimated using Euler-Bernoulli beam model, assuming perfect fixity at the supported end, and with Young's modulus= 70GPa, are obtained as 6.62, 41.51, 116.24, 226.25, and 376.54rad/s, respec-

tively. The vibration data was acquired at a sampling rate of 2048samples/s, and passed through a band-pass filter of frequency range 2-1000Hz. Corresponding to each of the four measurements  $\{x_i(t)\}_{i=1}^4$  made, a normalized time function given by  $y_i(t) = \frac{x_i(t) - m_i}{\sigma_i}$  is defined. Here  $m_i$  and  $\sigma_i$  are, respectively, the expected value and standard deviation of  $x_i(t)$ . This normalized data was subjected to the extreme value analysis. Some of the results from this study are shown in figures 9(b) and (d). From these figures, we can conclude that the extreme responses belong to the Gumbel domain of attraction for beam with and without the presence of wires. The estimates of extreme response over a time duration of 0.5s and with 500 samples are shown in figures 9(c) and (e). These figures also show the empirical PDF of extremes estimated using an extended ensemble of response time histories leading to 5000 samples of extrema. The empirical PDFs seem to compare well with the data obtained from Gumbel model estimated with limited samples.

It may be emphasized in the context of this example that the performance functions that have been studied here are related to quantities that are actually measured. It is possible that there could be other performance functions of interest that may be related to the quantities that are not directly measured or are difficult to measure. This leads to an interesting question on the possibility of estimating reliability, based on measurements of certain accessible variables, with respect to quantities that are not measured. For instance, in the beam structure (figure 9(a)), based on the measured acceleration response, one could estimate the probability of the event that the beam would yield near the support (as per, say, the Von Mises criterion). It seems possible to answer questions of this kind by combining the reliability analysis framework discussed in this paper with methods of dynamic state estimation. Here it becomes essential to postulate a mathematical model for the vibrating system. To clarify this point, we consider a randomly excited sdof system, and assume that the measurements have been made on the displacement response. The governing equation (termed as the process equation) is obtained as

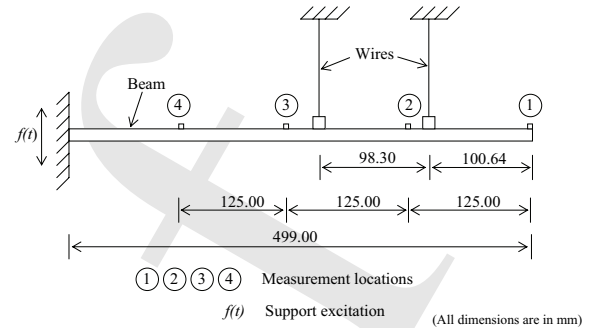


Fig. 9 (a)

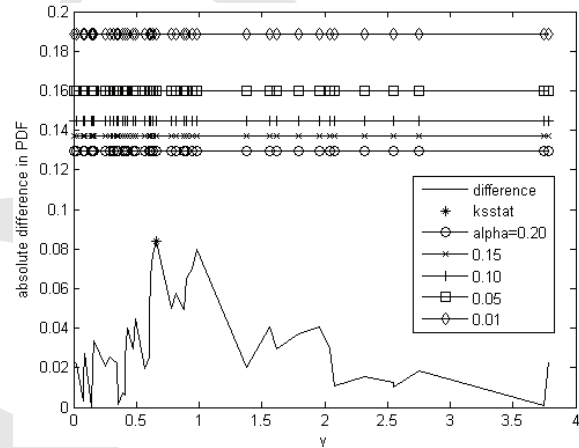


Fig. 9 (b)

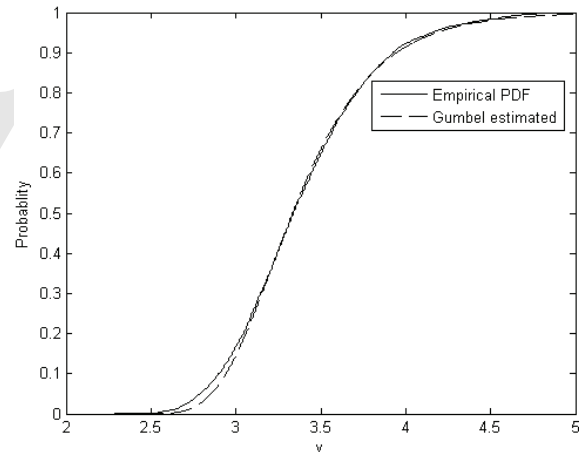


Fig. 9 (c)

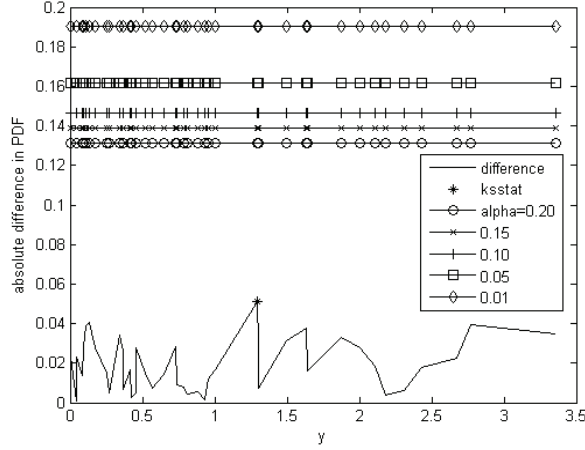


Fig. 9 (d)

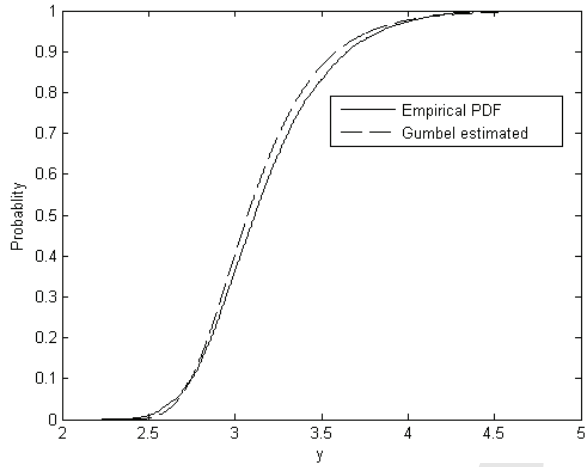


Fig. 9 (e)

Figure 9: Reliability analysis using experimentally measured data; (a) cantilever beam supported on wires; (b) results of the K-S test (beam without wire); (c) PDF of extreme displacement  $y_3(t)$  (beam without wire); (d) results of the K-S test (beam suspended by wires); (e) PDF of extreme displacement  $y_3(t)$  (beam suspended by wires).

$$\begin{cases} \dot{x}_1 \\ \dot{x}_2 \end{cases} = \begin{bmatrix} 0 & 1 \\ -\omega^2 & -2\eta\omega \end{bmatrix} \begin{cases} x_1 \\ x_2 \end{cases} + \begin{cases} 0 \\ \frac{f(t)}{m} \end{cases} + \begin{cases} 0 \\ \xi(t) \end{cases} \quad (51)$$

Here  $\xi(t)$  is the process noise, and  $f(t)$  is the external excitation. The measurement equation is

given by

$$y(t) = x(t) + \zeta(t) \quad (52)$$

Here  $\zeta(t)$  is the measurement noise. We model the noise terms  $\xi(t)$  and  $\zeta(t)$  as zero mean, stationary Gaussian random processes. We consider a performance function related to the highest reaction transferred to the support, although we have not been able to measure this force. The idea here is to estimate the ‘hidden’ variable, that is, the reaction

$$\hat{R}(t) = \omega^2 \hat{x}_1(t) + 2\eta\omega \hat{x}_2(t) \quad (53)$$

where a hat over a variable indicates the estimate of the corresponding state after the information contained in the measurement  $y(t)$  has been assimilated. Such estimates can be obtained by using the well known Kalman filtering techniques for the class of linear dynamical systems carrying Gaussian additive noises (Brown and Hwang 1992). For the purpose of illustration we consider the system with  $\eta = 0.08$ ,  $\omega = 2\pi\text{rad/s}$  and  $T = 35\text{s}$  and mimic numerically a measurement situation. The process and measurement noises  $\xi(t)$  and  $\zeta(t)$  are taken to be independent with standard deviations of  $0.04\text{N}$  and  $0.02\text{m}$ , respectively. The forcing function  $f(t)$  is modeled as a zero mean, stationary white Gaussian random process with a strength of  $1.0\text{N}^2$ . We discretize the governing stochastic differential equation (as in section 4.2). The measurement  $y(t)$  is obtained numerically, and is seeded with random Gaussian noise sequence  $\zeta(t)$  (equation 52). Based on the Kalman filter algorithm, the estimate of  $\hat{R}(t)$  is obtained using equation 53. This is repeated for all episodes of measurements. The resulting ensemble of  $\hat{R}(t)$  is subsequently used in the extreme value analysis, and the results from this exercise are shown in figure 10. Here the  $W$  statistic in the Hasofer-Wang test is obtained as 21.5 ( $N = 3583$  and  $k = 89$ ) that lead to the acceptance of the null hypothesis at 5% significance level. The parameters of the Gumbel PDF are subsequently estimated using 500 samples of  $\hat{R}(t)$ , and the resulting PDF is marked as ‘Gumbel model’ in figure 10. This result is compared with the empirical PDF obtained with 5000 samples of  $R(t)$ . The

mutual agreement between these two PDFs points towards the acceptability of proposed procedure.

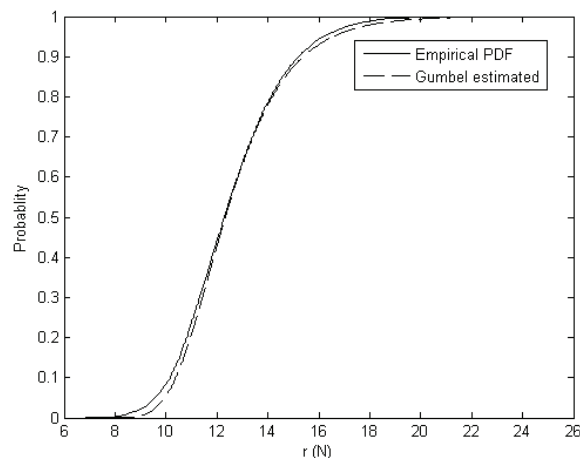


Figure 10: Reliability analysis with respect to an unmeasured response variable in an existing structure; PDF of extreme of reaction transferred to the support.

## 6 Discussion and closing remarks

The primary objective of this investigation has been to combine Monte Carlo simulation methods with statistical inference methods on extreme values to estimate the PDF of the extremes of response of nonlinear dynamical systems driven by white Gaussian noise excitations. Illustrative examples of reliability analysis of a wind turbine structure based on numerical simulations, and reliability analysis of a nonlinear beam, based on experimentally measured data are also discussed. The study draws on the works that exist in the mathematical literature on the determination of domain of attraction of extreme value distribution based on the availability of limited observation data. In the present study the “observation” data is taken to be the results of Monte Carlo runs of the governing structural dynamics model. While the limitation on available data is natural in the context of extremes of environmental processes such as earthquake, wind and floods, in the present study this limitation is artificially enforced as resulting from a perceived inability to perform large number of Monte Carlo simulation runs on the structural models. This can be

considered to be a reasonable view point especially when dealing with prediction of reliability of large scale engineering structures, such as nuclear power plant structures, in which, the typical probability of failure could be of the order of  $10^{-5}$  or even less. The proposed method consists of a two level simulation exercise. In the first, a few samples of response time histories are generated, and all the extremes from these time histories are employed to test the hypothesis on the basin of attraction of extremes to which the data belongs. Subsequently, another set of simulations are performed wherein the highest response over a given time duration and across an ensemble is obtained. Based on this data the parameters of the appropriate extreme value PDF are estimated. The resulting PDF is used for assessment of the structural reliability. The sample size in the two stages of simulation is largely independent of the value of reliability that the model aims to evaluate. The proposed procedure thus enables the evaluation of structural reliability with relatively less computational effort. To clarify this point further, on a Pentium 2.4GHz 512MB RAM machine, the computation time for the determining the extreme value distribution of the response of the Duffing system considered in section 5.2, by Monte Carlo simulations using 5000 samples, was 80min 27s, while the time to compute the same using the proposed procedure using 100samples was 2min 21s. In this sense the proposed method aims to achieve what the methods based on variance reduction schemes aim to achieve, albeit on an entirely different basis.

The following observations can be made based on the study conducted in this work.

- The range of numerical examples considered in this study covers stochastic response of linear and nonlinear sdof and mdof systems, and of large scale models (such as the wind turbine structure) and structures investigated using experimental techniques. The use of white Gaussian model as an excitation source is not restrictive since other forms of spectral content could easily be accommodated by adding additional filters. The Gumbel and Weibull models are useful models

for PDF of the extreme structural responses. The results from this study are compared with the results from out-crossing models for a class of problems. The proposed method compares well with the results from large scale Monte Carlo simulations.

- In most cases the tests proposed by Galambos, Pickands and Hasofer-Wang are observed to lead to consistent results on the forms of the extreme value PDFs, with the exception being the case of dynamical systems that possess limit cycle behavior. In these cases (section 5.2), the Galambos and Hasofer-Wang methods seem to consistently contradict the result from the Pickands method. This aspect of the results remain unexplained in this study, and it requires further investigation.
- The study assumes the validity of the classical forms of extreme value distributions, although it is well known that these distributions are generally valid only for iid sequences of random variables. These forms could be still applicable only when the random variable sequences satisfy certain conditions on the nature of their mutual dependency. The authors are not aware of any statistical tests to ascertain if a given set of data indeed satisfy such requirements. This aspect also requires further investigation. In this context it must be emphasized that while the study does not take into account the effect of dependency characteristics of the random sequence on the form of asymptotic extreme value distribution, in the determination of the model parameters such dependency characteristics are indeed automatically taken into account. The study does not make any specific assumptions such as independence of crossings and Poisson models for number of level crossings, as is usually done in the available analytical models for extremes.
- The proposed method could be implemented as a component in the seismic fragility analysis of large scale structures. This has particu-

lar advantages since for the proposed method issues such as structural nonlinearity, non-Gaussian nature of loads/responses and the size of the structure are not impediments in its implementation.

- In situations where the structure under investigation is not easily amenable for mathematical modeling, as for example, in the case of seismic safety assessment of structures with electronic components or other “active” components, one often takes recourse to qualification testing. This is true in the field of earthquake engineering, and for power plant components and equipment. As has been illustrated, the proposed method has the potential for applications in these situations also. This however would call for more detailed test procedures than what perhaps is considered adequate in a typical qualification test. These aspects again require further investigation.

**Acknowledgement:** CSM wishes to thank the Board of Research in Nuclear Sciences, Department of Atomic Energy, Government of India for the financial support received to carry out a part of this work.

## References

- Ahlstrom, A.** (2005): *Aeroelastic simulation of wind turbine dynamics*, PhD thesis, Department of mechanics, Royal Institute of Technology, Sweden.
- Alves, I.F.; Neves, C.** (2006): Testing extreme value conditions- an overview and recent approaches, *International Conference on Mathematical Statistical Modeling in honor of E Castillo*, June 28-30, 1-16.
- Au, S.K.; Beck, L.L.** (2001): First excursion probabilities for linear systems by very efficient importance sampling, *Probabilistic Engineering Mechanics*, 16, 193-207.
- Brown, R.G.; Hwang, P.Y.C.** (1992): *Introduction to random signals and applied Kalman filtering*, John Wiley & Sons, New York.

- Bayer, V.; Bucher, C.G.; Dorka, U.E.** (1999): First passage reliability of bridges by spectral importance sampling, *Structural Dynamics-EURODYN*, (Eds: L Fryba, and J Naprstek,), Balkema, Rotterdam, 237-242.
- Brenner, C.E.; Bucher, C.G.** (1995): A contribution to the SFE-based reliability assessment of nonlinear structures under dynamic loading, *Probabilistic Engineering Mechanics*, 10, 265-273.
- Cai, G.Q.; Lin, Y.K.** (1998): Reliability of nonlinear frame under seismic excitation, *Journal of Engineering Mechanics ASCE*, 124(8), 852-856.
- Castillo, E.** (1988): *Extreme value theory in engineering*, Academic Press, Boston.
- Coles, S.** (2001): *An introduction to statistical modeling of extreme values*, Springer.
- Dunne, J.F.; Ghanbari, M.** (2001): Efficient extreme value prediction for nonlinear beam vibrations using measured random response histories, *Nonlinear dynamics*, 24, 71-101.
- Galambos, J.** (1978): *The asymptotic theory of extreme order statistics*, John Wiley and Sons, New York.
- Galambos, J.** (1980): A statistical test for extreme value distributions, *Colloquia Mathematica Societatis Janos Bolyai*, 221-229.
- Galambos, J.** (1987): The selection of the domain of attraction of an Extreme value distribution from a set of data in Extreme Value Theory (proceedings of a conference held in Oberwolfach), Berlin: Springer Verlag, *Lecture notes in statistics*.
- Gan, C.B.; Zhu, W.Q** (2001): First-passage failure of quasi-non-integrable-Hamiltonian systems, *International Journal of Nonlinear Mechanics*, 36, 209-220.
- Gumbel, E.J.** (1958): *Statistics of extremes*, Columbia University Press, New York.
- Gupta, S.; Manohar, C.S.** (2006): Reliability analysis of randomly parametered linear vibrating systems subjected to stochastic excitations, *Journal of Sound and Vibration*, 297(3-5), 1000-1024.
- Gupta, S.; Manohar, C.S.** (2005): Development of multivariate extreme value distributions in random vibration applications, *Journal of Engineering Mechanics, ASCE*, 131(7), 712-720.
- Gupta, S.; Manohar, C.S.** (2004): Response surface method for time variant reliability analysis of nonlinear random structures under nonstationary excitations, *Nonlinear Dynamics*, 36, 267-280.
- Gupta, S.; Manohar, C.S.** (2003): An improved response surface method for the determination of failure probability and importance measures, *Structural Safety*, 26, 123-139.
- Hagen, O.** (1992): Conditional and joint failure surface crossing of stochastic processes, *Journal of Engineering Mechanics ASCE*, 118(9), 1814-1839.
- Hagen, O.;Tvedt, L.** (1991): Vector process out-crossing as parallel system sensitivity measure, *Journal of Engineering Mechanics ASCE*, 117(10), 2201-2220.
- Hasofer, A.M.A.;Wang, Z.** (1992): A test for extreme value domain of attraction, *Journal of the American Statistical Association*, 87(417), 171-177.
- IEC** (1998): *Wind Turbine Generator Systems Part 1: Safety Requirement, International Electrotechnical Commission (IEC)*, IEC/TC 88 61400-1, 2<sup>nd</sup> Edition, Geneva.
- Ibrahim, R.A.** (2005): *Liquid sloshing dynamics: theory and applications*, Cambridge University Press, Cambridge.
- Kiureghian, A.D.** (2000): The geometry of random vibrations and solutions by FORM and SORM, *Probabilistic Engineering Mechanics*, 15(1), 81-90.
- Klein, G.H.** (1964): Random excitation of a nonlinear system with tangent elasticity characteristics, *Journal of Acoustical Society of America*, 36(11), 2095-2105.
- Kloeden, P.E.; Platen, E.** (1999): *Numerical solution of stochastic differential equations*, Springer, Berlin.
- Kotz, S; Nadarajah, S.** (2000): *Extreme value distributions*, Imperial College Press, London.
- Leadbetter, M.R.;Lindgren, G.; Rootzen, H.** (1983): *Extremes and related properties of random sequences and processes*, Springer Verlag,

Berlin.

**Leira, B.J.** (2003): Extremes of Gaussian and non-Gaussian vector processes: a geometric approach, *Structural Safety*, 25, 401-422.

**Leira, B.J.** (1994): Multivariate distributions of maxima and extremes for Gaussian vector processes, *Structural Safety*, 14, 247-265.

**Li, R.; Ghanem, R.** (1998): Adaptive polynomial chaos expansion applied to statistics of extremes in nonlinear random vibration, *Probabilistic Engineering Mechanics*, 13(2), 125-136.

**Lillefors, H.W.** (1969): On the Kolmogorov-Smirnov test for exponential distribution with mean unknown, *Journal of American Statistical Association*, 64, 387-389.

**Lin, Y.K.; Cai, G.Q.** (1995): *Probabilistic structural dynamics*, McGraw-Hill, New York.

**Macke, M.; Bucher, C.** (2003): Importance sampling for randomly excited dynamical systems, *Journal of Sound and Vibration*, 268, 269-290.

**Manohar, C.S.** (1995): Methods of nonlinear random vibration analysis, *Sadhana*, 20, 345-371.

**Manohar, C.S.; Gupta, S.** (2005): Modeling and evaluation of structural reliability: current status and future directions, in *Recent Advances in Structural Engineering*, Edited by K S Jagadish and R N Iyengar, University Press, Hyderabad, pp. 90-187.

**Melchers, R.E.** (1999): *Structural Reliability Analysis and Prediction*, Second edition, John Wiley, Chichester.

**Nigam, N.C.** (1983): Introduction to random vibrations, MIT Press, Cambridge. **Noori, M.; Dimentberg, M.; Hou, Z.; Christodoulidou, R.; Alexandrou, A.** (1995): First-passage study and stationary response analysis of a BWB hysteresis model using quasi-conservative stochastic averaging, *Probabilistic Engineering Mechanics*, 10, 161-170.

**Olsen, J.I.; Naess, A.** (2006): Estimation of failure probability of linear dynamical systems by importance sampling, *Sadhana*, 31(4), 429-443.

**Oye, S.** (1996): *Flex4: Simulation of Wind Turbine Dynamics*, in B M Pedersen (Ed), State of the art of aeroelastic codes for wind turbine cal-

culations, 71-76, Lyngby, Denmark.

**Pickands J.III.** (1975): Statistical inference using extreme order statistics, *Annals of statistics*, 3, 119-131.

**Pradlwarter, H.J.; Schueller, G.I.** (1999): Assessment of low probability events of dynamical systems by controlled Monte Carlo simulation, *Probabilistic Engineering Mechanics*, 14, 213-217.

**Rackwitz, R.** (1998): Computational techniques in stationary and non-stationary load combination: A review and some extension, *Journal of Structural Engineering*, 25(1), 1-20.

**Rice, S.O.** (1956): A mathematical analysis of noise, in N Wax (Ed.), Selected papers in random noise and stochastic processes, *Dover Publications*, 133-294.

**Roberts, J.B.** (1986): First passage probabilities for randomly excited systems: diffusion methods, *Probabilistic Engineering Mechanics*, 1, 66-81.

**Sharp, W.D.; Allen, E.J.** (1998): Numerical solution of first passage problems using an approximate Chapman-Kolmogorov relation, *Probabilistic Engineering Mechanics*, 13(3), 233-241.

**Song, J.; Kiureghian, A.D.** (2006): Joint failure probability and reliability of systems under stochastic excitations, *Journal of Engineering Mechanics*, ASCE, 132(1) 65-77.

**Veneziano, D.; Grigoriu, M.; Cornell, C.A.** (1977): Vector process models for system reliability, *Journal of Engineering Mechanics*, ASCE, 103(EM3), 441-460. **Wen, Y.K.** (1986): Stochastic response and damage analysis of inelastic structures, *Probabilistic Engineering Mechanics*, 1(1), March 1986, Pages 49-57.

**Yao, T.H.J.; Wen, Y.K.** (1996): Response surface method for time-variant reliability analysis, *Journal of Structural Engineering*, ASCE, 122(2), 193-201.

**Zhao, Y.G.; Ono, T.; Idota, H.** (1999): Response uncertainty and time-variant reliability analysis for hysteretic mdof structures, *Earthquake Engineering and Structural Dynamics*, 28, 1187-1213.

Proof